NATIONAL ADVISORY COMMITTEE FOR AERONAUTICS

TECHNICAL NOTE 4353

EXPLORATORY WIND-TUNNEL INVESTIGATION AT HIGH SUBSONIC AND TRANSONIC SPEEDS OF JET FLAPS ON UNSWEPT RECTANGULAR WINGS

By Vernard E. Lockwood and Raymond D. Vogler

Langley Aeronautical Laboratory
Langley Field, Va.

NACA

Washington
August 1958

NATIONAL ADVISORY COMMITTEE FOR AERONAUTICS

TECHNICAL NOTE 4353

EXPLORATORY WIND-TUNNEL INVESTIGATION AT HIGH SUBSONIC AND TRANSONIC SPEEDS OF JET FLAPS ON UNSWEPT RECTANGULAR WINGS

By Vernard E. Lockwood and Raymond D. Vogler

SUMMARY

An investigation has been made in the Langley high-speed 7- by 10-foot tunnel by means of the transonic-bump technique to determine the lift augmentation of several jet-flap configurations. Thrust-recovery characteristics of some of the thick-wing configurations were also determined. The investigation covered a Mach number range from 0.40 to 1.10, and a maximum momentum coefficient of 0.30 was obtained at a Mach number of 0.40.

The results of the investigation indicated that the lift can be increased at any Mach number by blowing downward through a number of closely spaced holes along and near the trailing edge of the wing. The ratio of induced circulation lift to the lift component of the jet reaction increased with Mach number up to high subsonic speeds and then decreased through the transonic speed range. The induced circulation lift was greatly reduced when the jet location was moved from near the trailing edge to the 73-percent-chord line. A jet-augmented flap which used blowing from a slot on the upper surface in combination with a round trailing edge lost its effectiveness at Mach numbers of 0.60 or greater.

A 16-percent-thick wing with blowing rearward from a slot at the trailing edge showed a drag reduction about equivalent to the jet momentum throughout the Mach number range investigated. In contrast to this, a wing of similar geometry but with blowing from slots on the upper and lower surfaces near the maximum-thickness point showed drag reductions that were less than the jet reaction at transonic Mach numbers.

INTRODUCTION

Some recent low-speed investigations on jet flaps (refs. 1 to 4) have shown that remarkably high lift coefficients are obtainable by directing a thin high-velocity jet sheet of air downward at or near the

trailing edge of a wing. These arrangements are representative of integrated wing-engine installations where all or a large percentage of the exhaust products are used for combined thrust and lift augmentation. An exploratory type of investigation has been made to determine the aerodynamic characteristics at transonic speeds of some of these jet-flap arrangements that appear promising at low speeds. The investigation had a twofold purpose: to determine the extent of lift augmentation at transonic speeds and to determine whether jet flaps offer possibilities of drag reduction on blunt-wing profiles. This investigation was made in the Langley high-speed 7- by 10-foot tunnel by using the transonic bump to obtain Mach numbers from 0.40 to 1.10. Lift, drag, and pitching-moment data were obtained at angles of attack of -4°, 0°, and 4° for most configurations through a range of momentum coefficients varying from 0 to 0.30 at a Mach number of 0.40 and from 0 to 0.03 at a Mach number of 1.10.

The results of a similar investigation recently made in France are reported in reference 5.

SYMBOLS

The data are presented with respect to the wind axes, with the origin on the wing root chord 1 inch behind the leading edge (figs. 1 and 2), which resulted in the moment center being located at different percentages of the wing chord as shown in figures 3 and 4.

C_L lift coefficient, $\frac{2(\text{Semispan lift})}{qS}$

C_D drag coefficient, $\frac{2(\text{Semispan drag})}{qS}$

C_m pitching-moment coefficient, $\frac{2(\text{Semispan pitching moment})}{qSc}$

ΔC_L incremental lift coefficient, $(C_L)_{\text{total}} - (C_L)_{C_\mu=0}$

ΔC_D incremental drag coefficient, $(C_D)_{\text{total}} - (C_D)_{C_\mu=0}$

C_μ momentum coefficient, $\frac{w_j V_j}{gq\frac{S}{2}}$

S twice wing area of semispan model, sq ft

b	twice wing span of semispan model, ft
c	wing chord, ft
A	aspect ratio, b^2/S
t	airfoil thickness, ft
q	free-stream dynamic pressure, $\frac{\rho V^2}{2}$, lb/sq ft
ρ	free-stream density, slugs/cu ft
V	free-stream velocity, ft/sec
w_j	weight rate of air flow through jet holes or slots on semispan wing, lb/sec
g	acceleration due to gravity, 32.2 ft/sec^2
V_j	jet-exit velocity, assuming isentropic expansion to free-stream static pressure, $\sqrt{\frac{2\gamma}{\gamma - 1} RTg\left[1 - \left(\frac{p}{p_t}\right)^{\frac{\gamma-1}{\gamma}}\right]}$, ft/sec
γ	ratio of specific heats for air, 1.4
R	universal gas constant, $\frac{\text{ft-lb}}{\text{lb}}$ per deg Rankine
T	plenum-chamber stagnation temperature, deg Rankine
p	free-stream static pressure, lb/sq ft
p_t	total pressure in plenum chamber, lb/sq ft
M	Mach number
M_l	local Mach number
α	angle of attack of wing-chord plane, deg
δ	jet-deflection angle relative to wing chord plane, positive downward, deg

MODELS AND APPARATUS

This investigation utilized two basic wing profiles, one having a conventional NACA 65A004 airfoil section and the other a built-up section. The forward 75 percent of the built-up section was composed of the forward 28.3 percent of a 10.6-inch-chord NACA 65A006 airfoil; the rear 25 percent of the built-up section was wedge shaped. All other wing contours tested were modifications of the two basic profiles. The two basic wings had a semispan of 6.67 inches and a chord of 4.00 inches, resulting in an aspect ratio of 3.33, and thickness ratios of 4 percent and 15.6 percent. All wings were unswept and had a taper ratio of 1.0. The basic wing profiles and modifications thereto which resulted in changes in wing thickness ratio, aspect ratio, and trailing-edge configuration are shown in figures 3 and 4. Figure 3 shows the models in which the air was directed downward for lift augmentation, and figure 4 shows the models in which the compressed air was directed rearward for drag reduction or thrust recovery.

The thin high-velocity jet sheet which is characteristic of the jet flap was obtained by having a slot along the full span for models 1, 6, and 7, through which the compressed air was ejected. On the other models, however, the high-velocity jet sheets were simulated by means of a row of small closely spaced holes, as indicated in figures 3 and 4. On the thick wing the compressed air was introduced through a steel tube which formed an integral part of the model, and on the thin wing the air was introduced through a rectangular spanwise passage and a series of connecting holes to the plenum chamber.

The air which was ejected from the model was metered through a sharp-edge-orifice flowmeter so that the weight flow of air was known at all times. All models were equipped with pressure tubes and thermocouples in the plenum chambers so that the static pressure and temperature of the air might be determined.

TESTS

The tests were made by using the transonic-bump technique in the Langley 7- by 10-foot tunnel. The models were attached to a five-component electrical strain-gage balance located beneath the bump surface. The tests were made over a Mach number range from 0.40 to 1.10 at the Reynolds numbers shown in figure 5 for the models with the maximum wing chord (4.00 inches). The variation of the local Mach number over the bump in the vicinity of the model location for several Mach numbers is shown in figure 6.

The momentum coefficient, which was based on the weight flow of air and the theoretical isentropic exhaust velocity, varied from about 0.30 at $M = 0.40$ to about 0.03 at $M = 1.10$, depending on the model configuration. The tests were made at angles of attack of 0° and $\pm 4^\circ$ through the momentum-coefficient range. The jet deflection angles are the average values obtained from a static calibration. The jet deflection angles were assumed to be constant throughout the angle-of-attack and Mach number range investigated.

RESULTS

The data obtained in the jet-flap investigation reported herein are presented in the following figures:

DISCUSSION

Two types of jet flaps for lift augmentation are represented in the data of figures 7 to 13. Model 1 is a configuration similar to those which gave large lift augmentations in the investigations reported in references 1 and 2. In this case the jet flap was obtained by ejecting compressed air through a thin slot on the upper surface of a wing near a round trailing edge. The air clings to the trailing edge until separation occurs. On models 2, 3, and 4 the air is ejected at an angle to the chord plane through a series of closely spaced holes. The holes were drilled close together with the idea of simulating a full-span slot; however, no tests were made to determine to what extent this arrangement simulated a slot. On models 5, 6, and 7 the air was ejected rearward to determine whether drag reductions greater than the thrust were obtainable.

The blowing momentum coefficients presented in this report generally represent a choked condition of the nozzle (slot or holes). There are some combinations of low momentum coefficients and low Mach numbers, however, for which the holes or slots are unchoked and the velocity of the free stream is about equal to the velocity of the jet. When the jet velocity is about equal to free-stream velocity, a net momentum

coefficient $C_\mu\left(1 - V/V_j\right)$ may be a better correlation factor than C_μ. Because of the preliminary nature of this investigation and its limited instrumentation, it has been necessary to use C_μ, since unknown and possibly large nozzle losses preclude the determination of the actual jet velocity other than by theoretical isentropic expansion to free-stream pressure. The values of momentum used to obtain the values of C_μ presented are probably larger than the actual momentum of the jet and should be taken into account when evaluating and comparing these data. It is believed, however, that the data are an indication of the jet-flap potentialities at transonic speeds.

The pitching-moment data are presented without discussion.

Lift

The lift data of figure 7 (model 1) with top-surface blowing from a full-span slot shows that this jet-flap arrangement is effective in producing lift at low speeds ($M = 0.40$) as would be expected from the results presented in references 1 and 2. At $M = 0.60$ or above, however, this arrangement was ineffective; the loss of lift probably results from failure of the jet to cling to the round trailing edge.

The variation of lift coefficient with momentum coefficient shown in figure 17 at $\alpha = 0^\circ$ for models 2, 3, and 4 at low Mach numbers is unlike the variations obtained from wings with full-span blowing-slot arrangements as in the investigations of references 3 and 4. The data presented in figure 17 show a low rate of lift-coefficient increase with momentum coefficient, followed by a rapidly increasing rate of lift with momentum, in constrast to the initial high rate of lift-coefficient increase obtained at low momentum coefficients in references 3 and 4. The models of references 3 and 4 have full-span blowing slots at or close to the trailing edge, whereas the models of this investigation have a series of closely spaced holes ahead of the trailing edge.

The chordwise position of the holes is an important factor; the data of figures 17(c) and 17(d) indicate that it would take greater momentums to produce a given lift as the position of blowing is moved forward from the trailing edge.

A comparison of the lift-producing capabilities of models 2, 3, and 4 through the Mach number range is given in figure 18 in terms of the ratio of the induced circulation lift coefficient $\Delta C_L - C_\mu \sin \delta$ to the jet reaction component $C_\mu \sin \delta$. This ratio, which is often referred to as the "lift magnification factor," is presented for values of $C_\mu = 0.03$ and 0.06 at $\alpha = 0^\circ$. These data show that the lift

magnification increases with Mach number up to high subsonic speeds and then decreases through the transonic speed range. For example, model 4 with $C_\mu = 0.03$ gave a magnification factor which varied from about 1 at $M = 0.40$ to a high of about 7 at $M = 0.80$ and decreased to a value of about 3 at $M = 1.10$. These results are in general agreement with results presented in reference 5.

As was noted previously, the chordwise location of the blowing appears to be very important, as considerably less circulation lift is obtained from blowing at the 73-percent-chord line than from blowing at the 94-percent-chord line. The model with blowing at the 73-percent-chord line (model 3) gave little or no magnification at $M = 0.40$ but increased to a maximum value of about 4 at $M = 0.90$.

Drag

The drag coefficients with no blowing show a large range in magnitudes, as might be expected from the differences in thickness and contours of the various models (fig. 19). For example, the 19-percent-thick model 2 gave drag coefficients which varied from 23 times the value of model 3 at $M = 0.40$ to about 9 times the value of model 3 at $M = 1.10$. From the large values of drag coefficients obtained, it might be expected that blowing at or near the trailing edge would tend to reduce the basic drag coefficients. There is some evidence that this reduction does take place for model 5 at very low momentum coefficients (fig. 20). There is also evidence of drag reductions on lift model 2 at low momentum coefficients. (See figs. 8 and 9.) At Mach numbers of 0.40 and 0.60, significant reductions of drag occurred with only slight increases of lift. The 16-percent-thick model 6 with tangential blowing near the maximum thickness point (75-percent-chord) gave large thrust losses at transonic Mach numbers. It is possible that the loss of thrust is the result of shock-induced separation of the jet sheet from this thick wing, a condition which existed on the lift augmentation model 1. In contrast to the losses on model 6, model 7 gave relatively good thrust-recovery characteristics through the momentum coefficient and Mach number range investigated; that is, the drag reduction was about equivalent to the jet momentum from the trailing-edge slot.

SUMMARY OF RESULTS

An exploratory wind-tunnel investigation in the range of Mach numbers from 0.40 to 1.10 and momentum coefficients from 0 to 0.30 was made to determine the aerodynamic characteristics of unswept rectangular wings equipped with various jet-type flaps. The results are summarized as follows:

1. The jet-augmented flap which used blowing from a slot on the upper surface in combination with a round trailing edge lost its effectiveness at Mach numbers of 0.60 or greater.

2. The circulation lift, which was dependent on Mach number, was considerably increased by blowing downward through a number of closely spaced holes along and near the trailing edge. The ratio of the induced lift to the lift component of the jet reaction increased with Mach number, reaching a maximum value at high subsonic speeds, and then decreased through the transonic speed range.

3. The chordwise location of the blowing appears to be important on a jet-flap wing as ejection of the air at the 73-percent station gave considerably less induced circulation lift than the more rearward 94-percent location.

4. A 16-percent-thick wing with rearward air ejection through a slot at the trailing edge showed a drag reduction about equivalent to the jet momentum coefficient throughout the Mach number range investigated. In contrast to this, a wing with similar geometry but with blowing through slots on the upper and lower surface near the maximum-thickness point showed drag reductions that were less than the jet reaction through the transonic Mach number range.

Langley Aeronautical Laboratory,
National Advisory Committee for Aeronautics,
Langley Field, Va., June 13, 1958.

REFERENCES

1. Lockwood, Vernard E., Turner, Thomas R., and Riebe, John M.: Wind-Tunnel Investigation of Jet-Augmented Flaps on a Rectangular Wing to High Momentum Coefficients. NACA TN 3865, 1956.

2. Lowry, John G., and Vogler, Raymond D.: Wind-Tunnel Investigation at Low Speeds to Determine the Effect of Aspect Ratio and End Plates on a Rectangular Wing With Jet Flaps Deflected 85°. NACA TN 3863, 1956.

3. Williams, J., and Alexander, A. J.: Three-Dimensional Wind-Tunnel Tests of a 30° Jet Flap Model. C.P. No. 304, British A.R.C., 1957.

4. Malavard, L., Poisson-Quinton, Ph., and Jousserandot, P. (T. M. Berthoff and D. C. Hazen, trans.): Theoretical and Experimental Investigations of Circulation Control. Rep. No. 358, Dept. Aero. Eng., Princeton Univ., July 1956.

5. Poisson-Quinton, Ph., and Jousserandot, P.: Influence du soufflage an voisinage du bord de fuite sur les caractéristiques aérodynamiques d'une aile aux grandes vitesses. La Recherche Aéronautique (O.N.E.R.A.), no. 56, Feb. 1957, pp. 21-32.

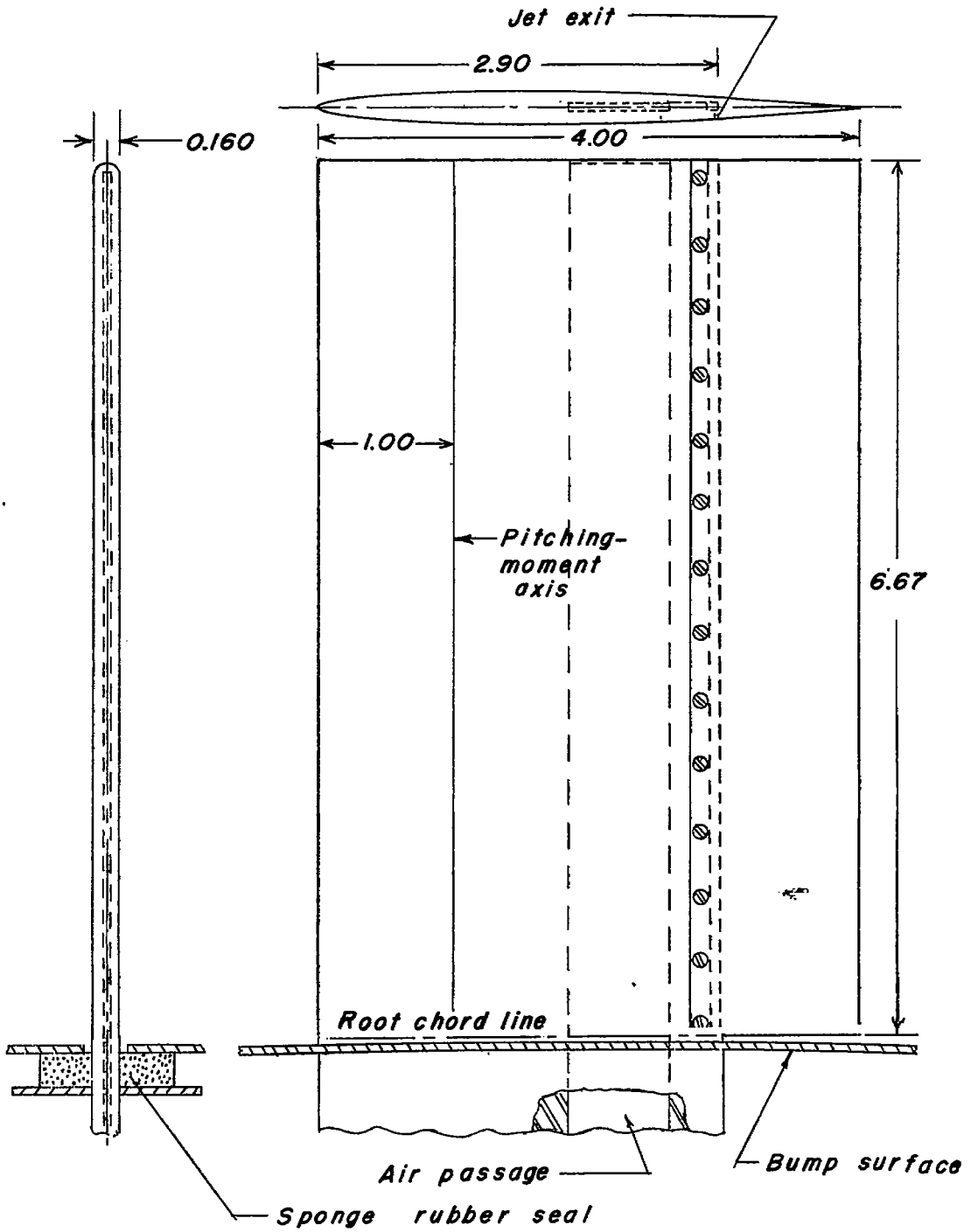

Figure 1.- Dimensions of the basic thin wing (model 3) with aspect ratio of 3.33. All dimensions are in inches.

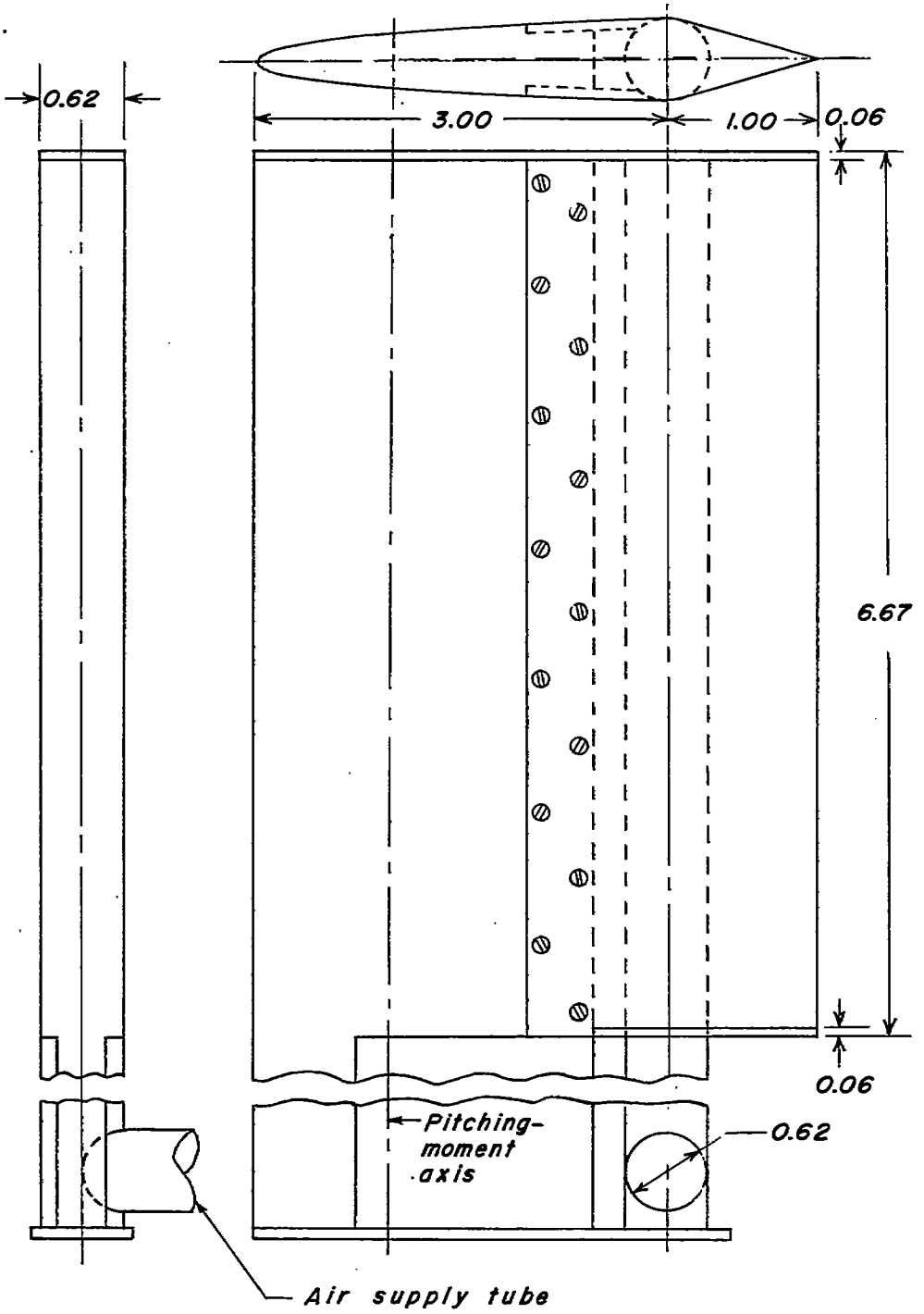

Figure 2.- Dimensions of the basic thick wing (model 7) with aspect ratio of 3.33. All dimensions are in inches.

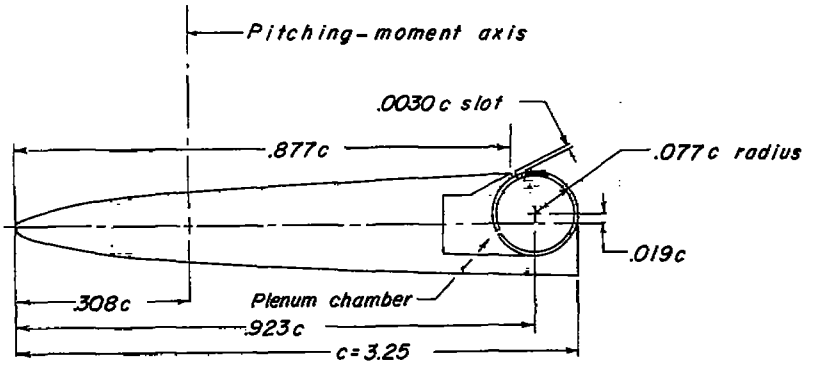

Model 1; A = 4.10; t = 0.192c.

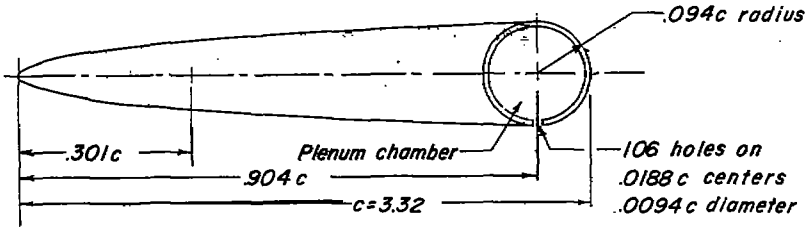

Model 2; A = 4.02; t = 0.188c.

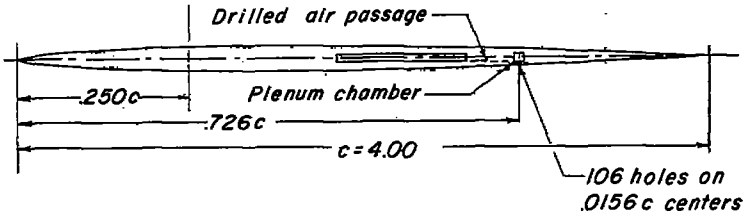

Model 3; A = 3.33; t = 0.040c.

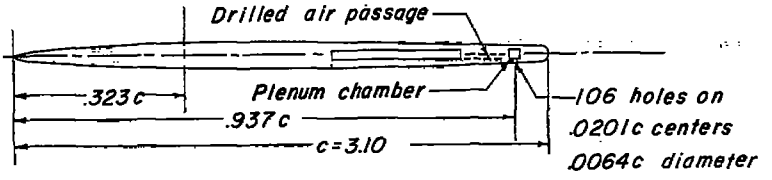

Model 4; A = 4.30; t = 0.052c.

Figure 3.- Contours of the various wings used in the jet-flap investigation.

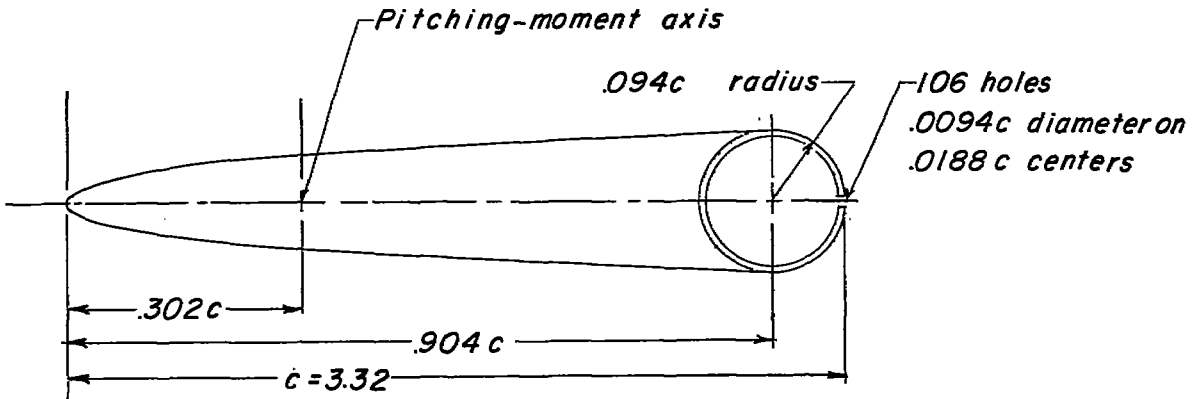

Model 5; A = 4.02; t = 0.188c.

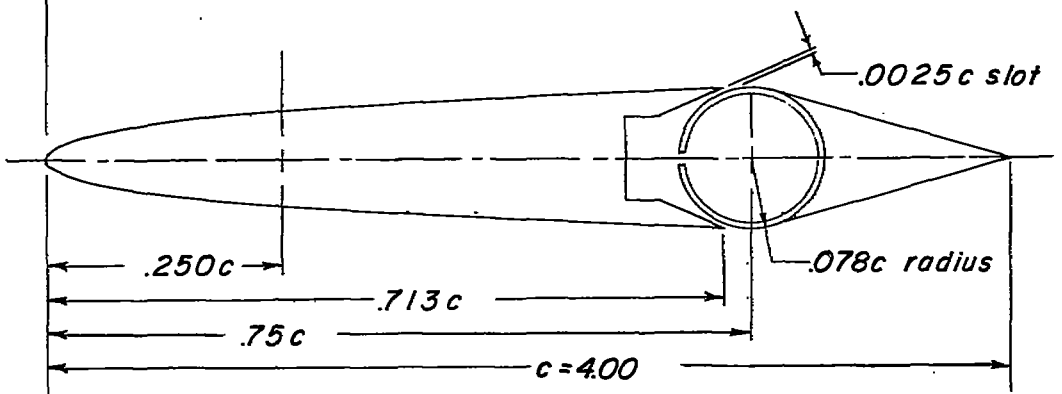

Model 6; A = 3.33; t = 0.156c.

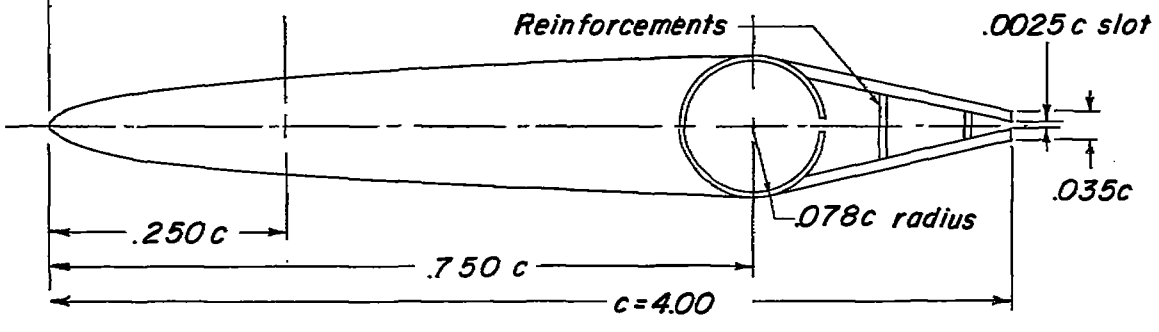

Model 7; A = 3.33; t = 0.156c.

Figure 4.- Contours of the various wings used in the undeflected-jet investigation.

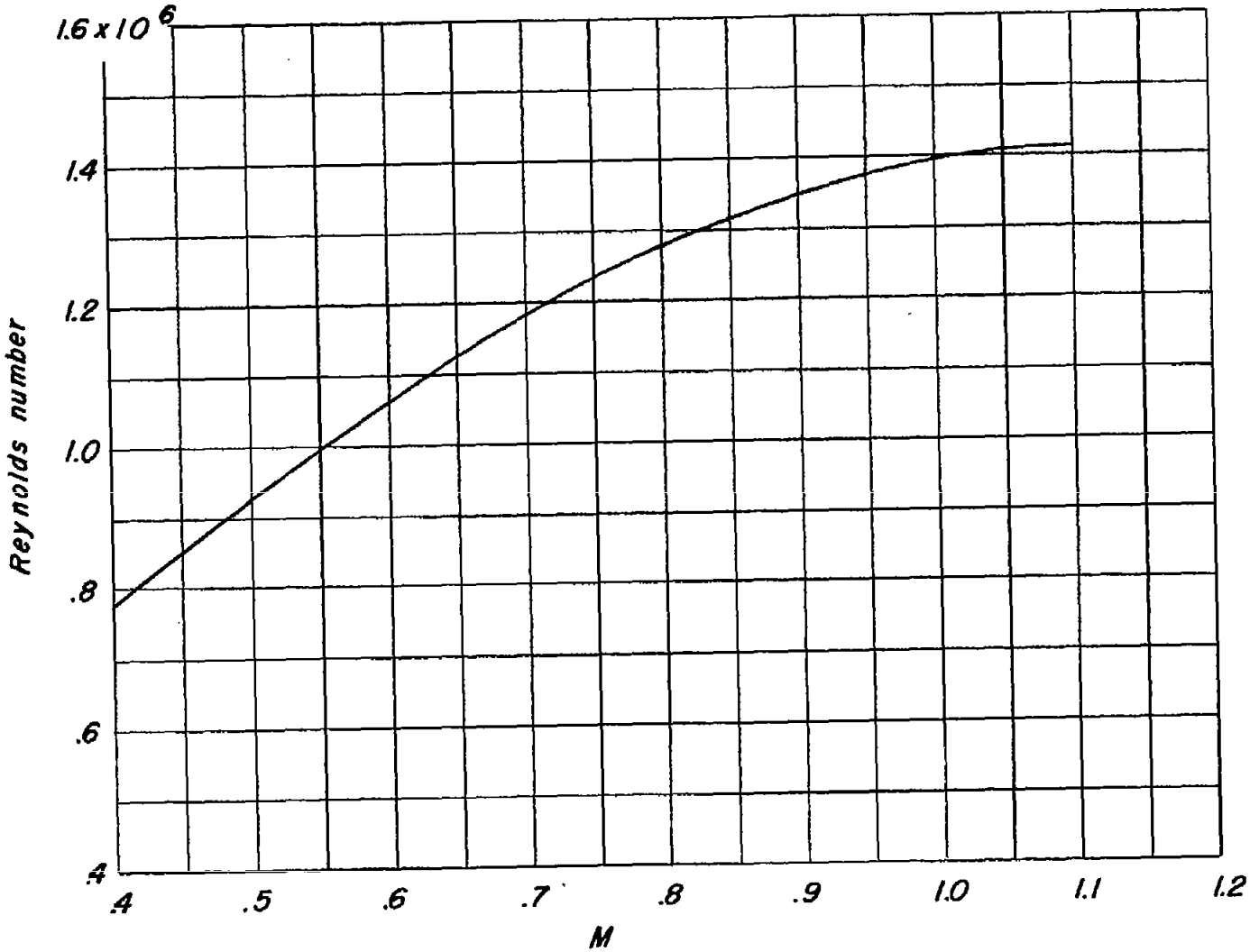

Figure 5.- Variation of mean test Reynolds number with Mach number for the wing with 4-inch chord.

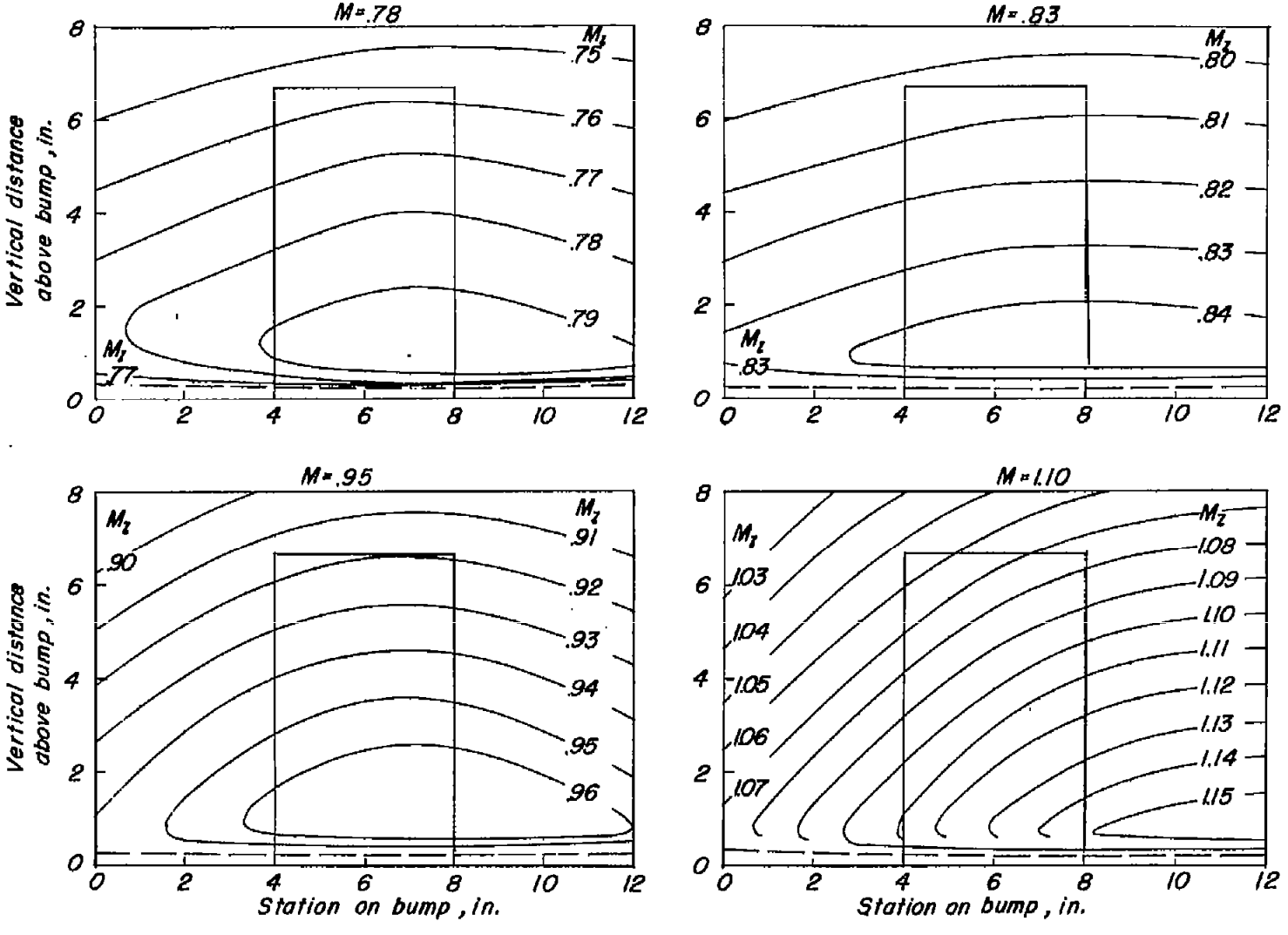

Figure 6.- Typical Mach number contours over transonic bump in region of model location. The boundary-layer thickness is indicated by the dashed lines.

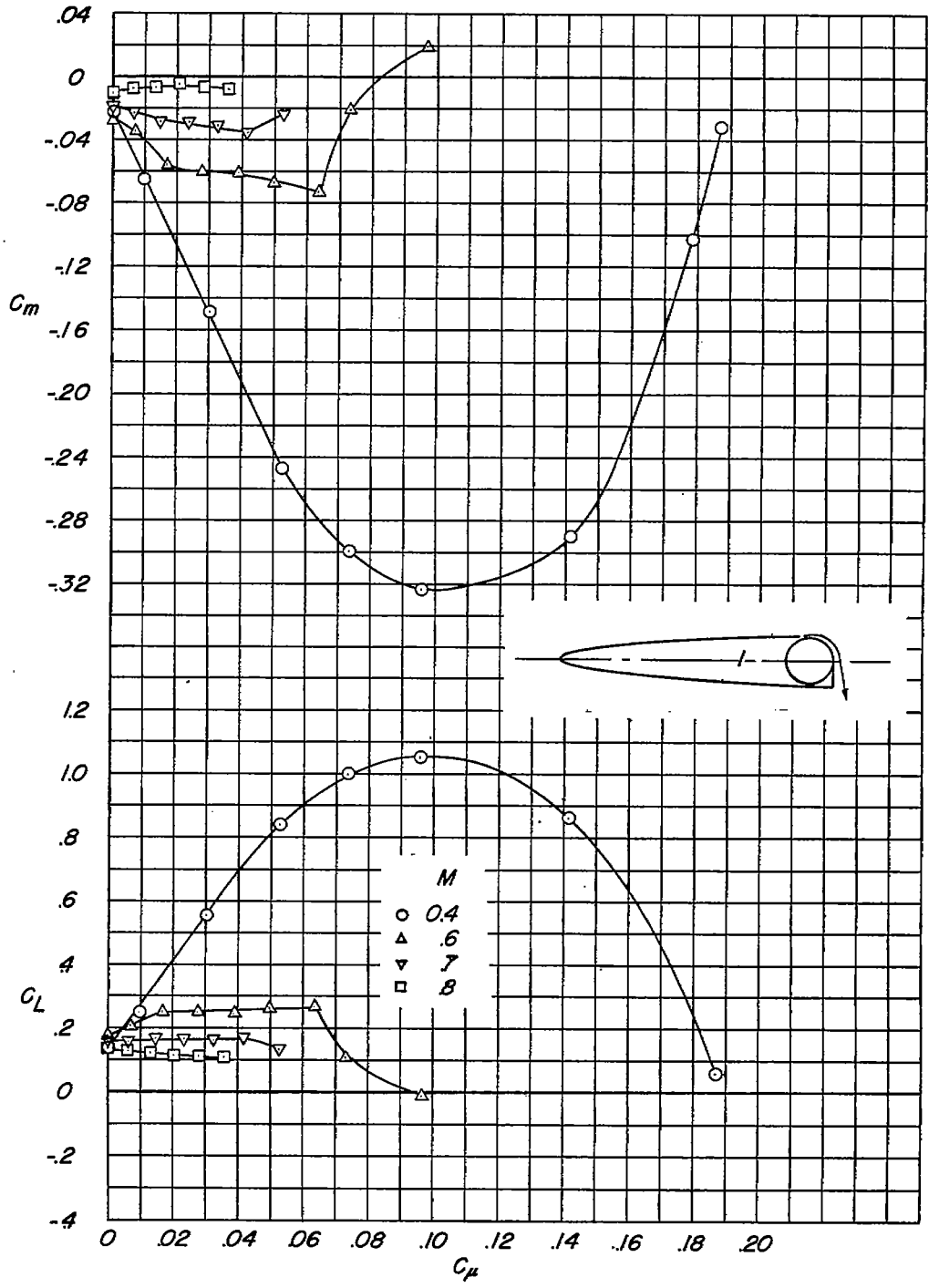

Figure 7.- Effect of Mach number on aerodynamic characteristics of jet-augmented-flap model 1. $\alpha = 0^\circ$; $\delta = 79.5^\circ$.

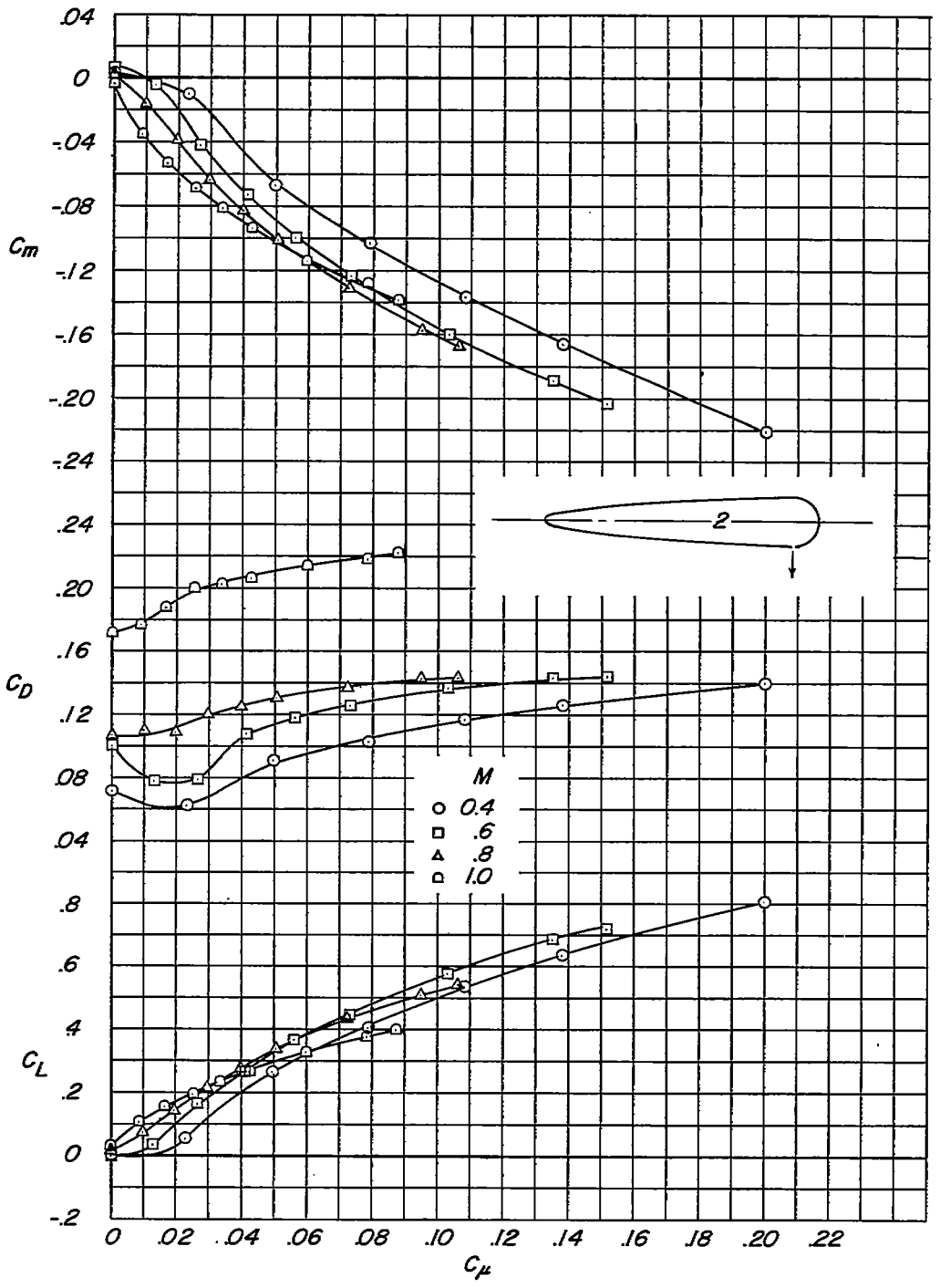

Figure 8.- Effect of Mach number on aerodynamic characteristics of jet-flap model 2. $\alpha = 0^\circ$; $\delta = 90^\circ$.

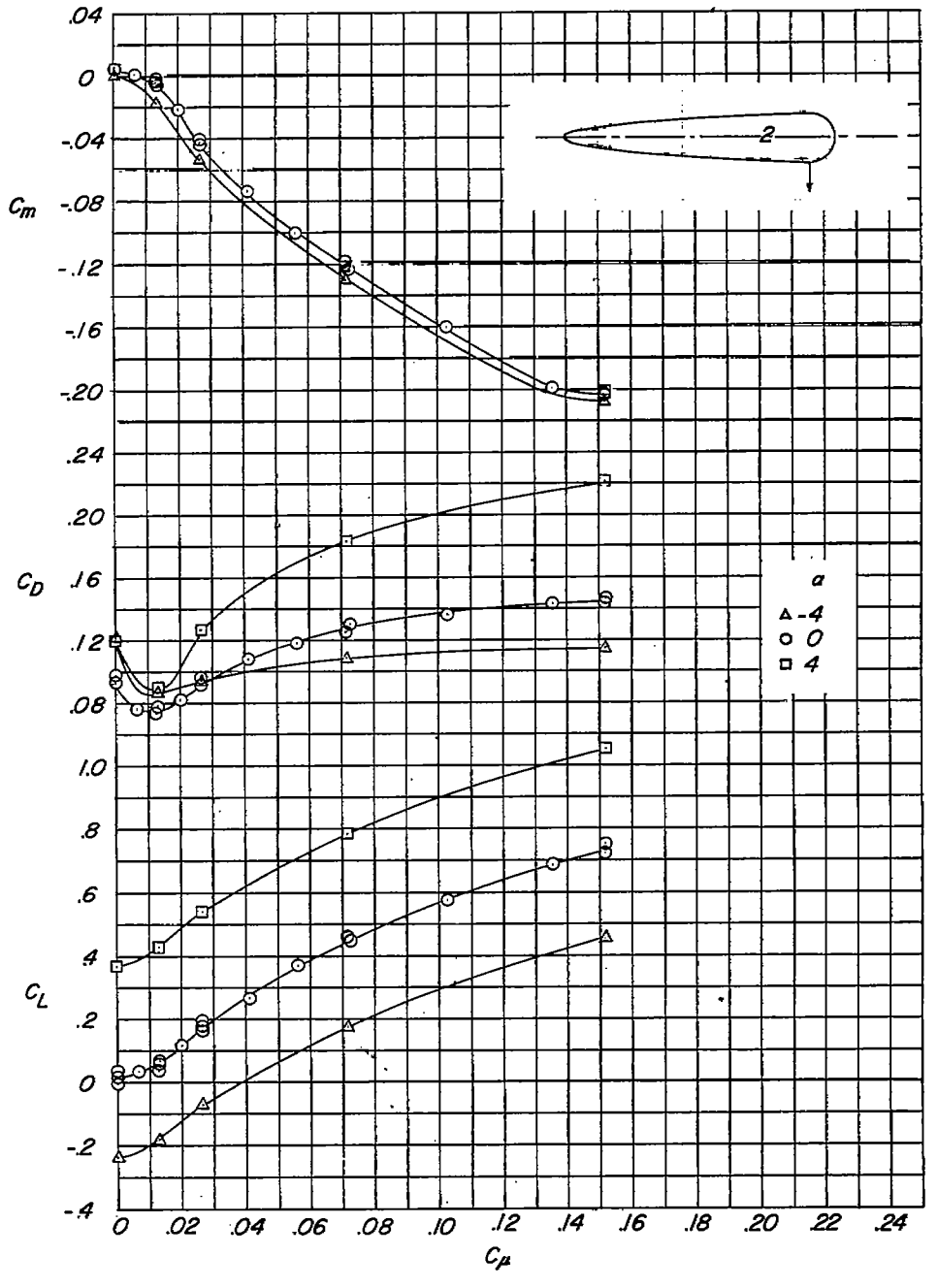

(a) $M = 0.60$.

Figure 9.- Effect of angle of attack on aerodynamic characteristics of jet-flap model 2. $\delta = 90^\circ$.

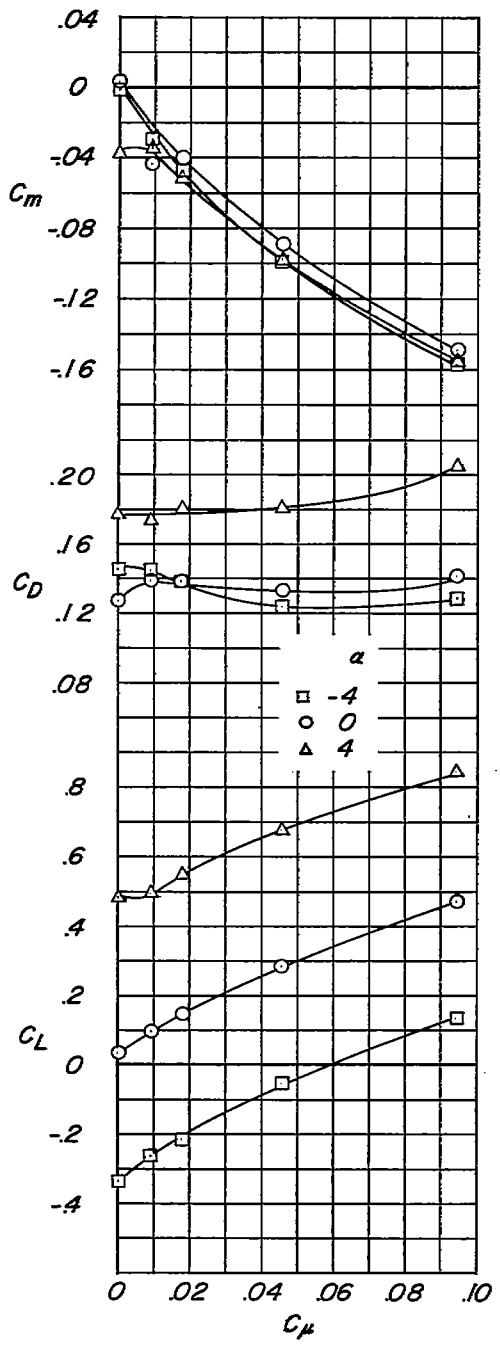

(b) M = 0.90.

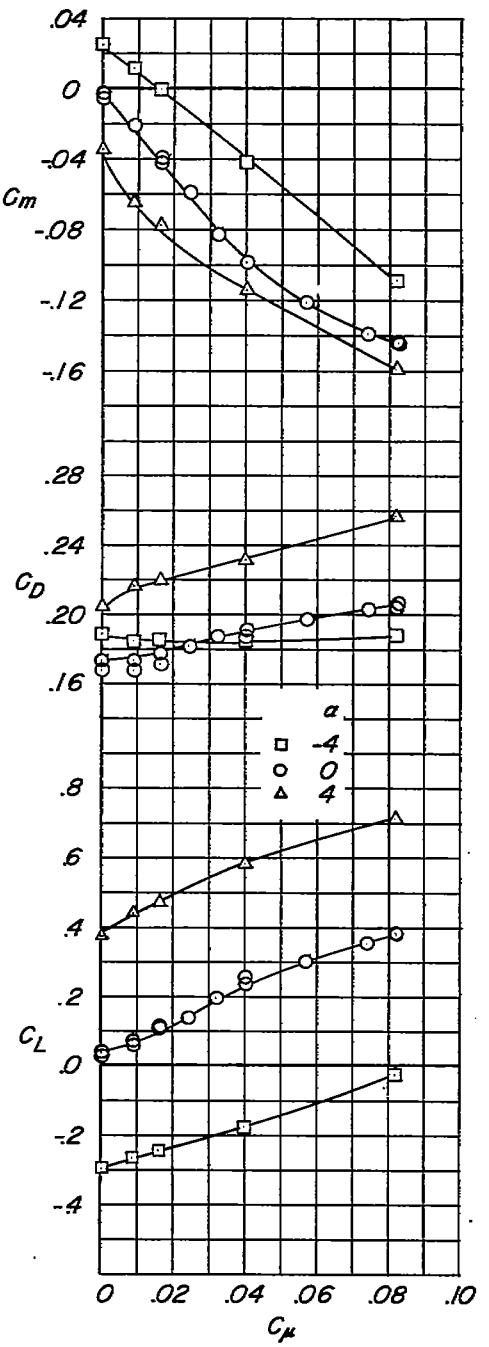

(c) M = 1.10.

Figure 9.- Concluded.

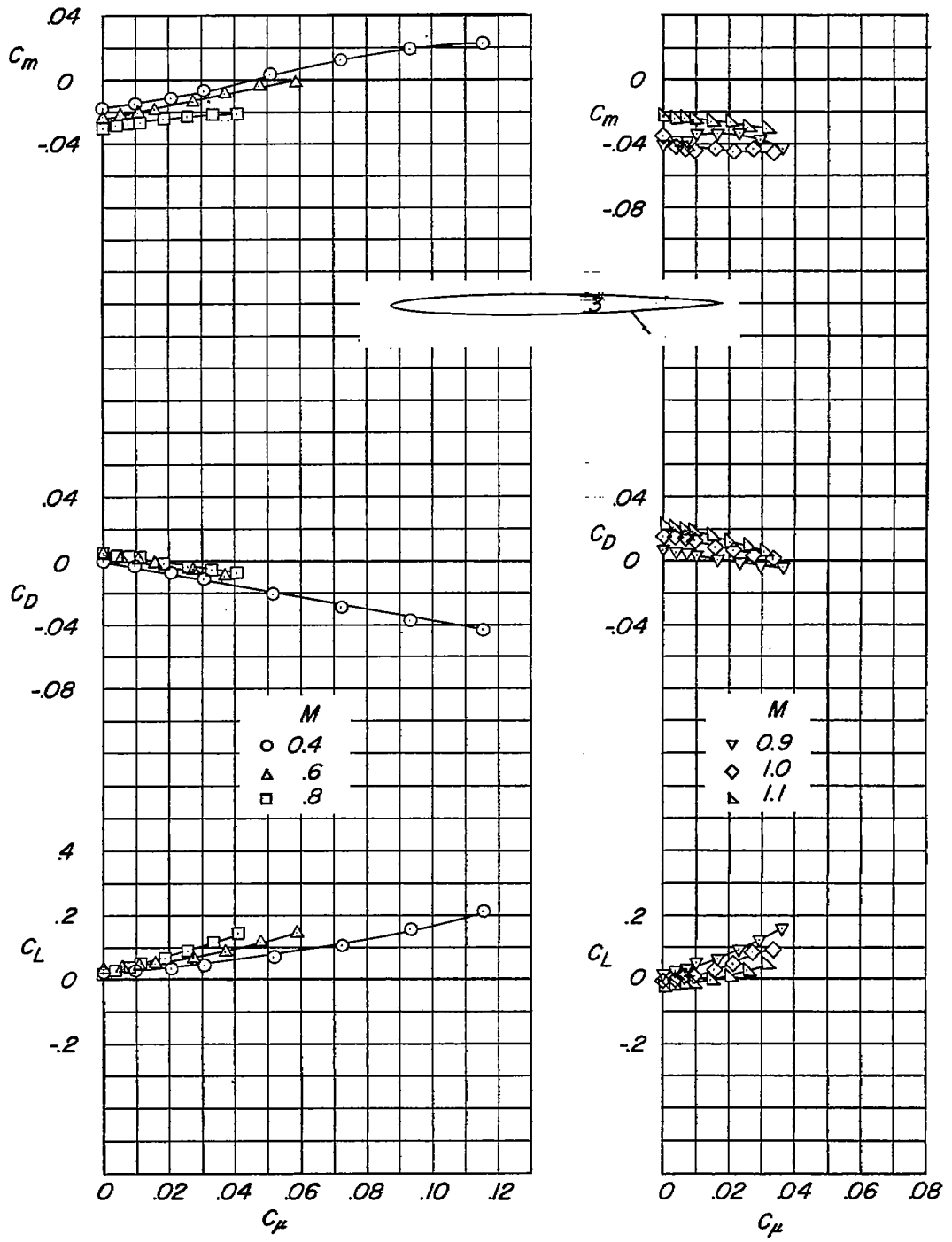

Figure 10.- Effect of Mach number on aerodynamic characteristics of jet-flap model 3. $\alpha = 0^\circ$; $\delta = 50^\circ$.

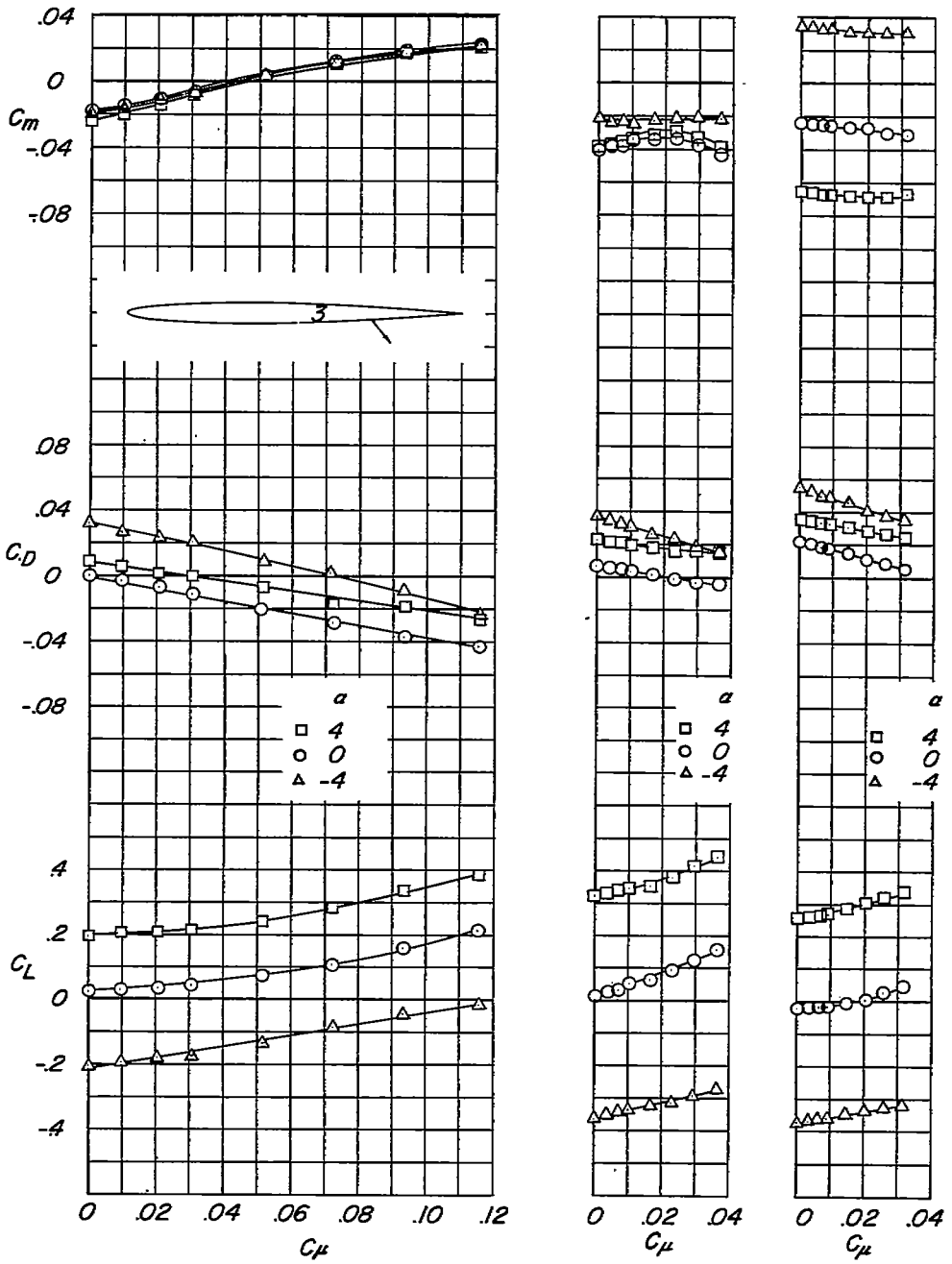

(a) M = 0.40. (b) M = 0.90. (c) M = 1.10.

Figure 11.- Effect of angle of attack on aerodynamic characteristics of jet-flap model 3. $\delta = 50^\circ$.

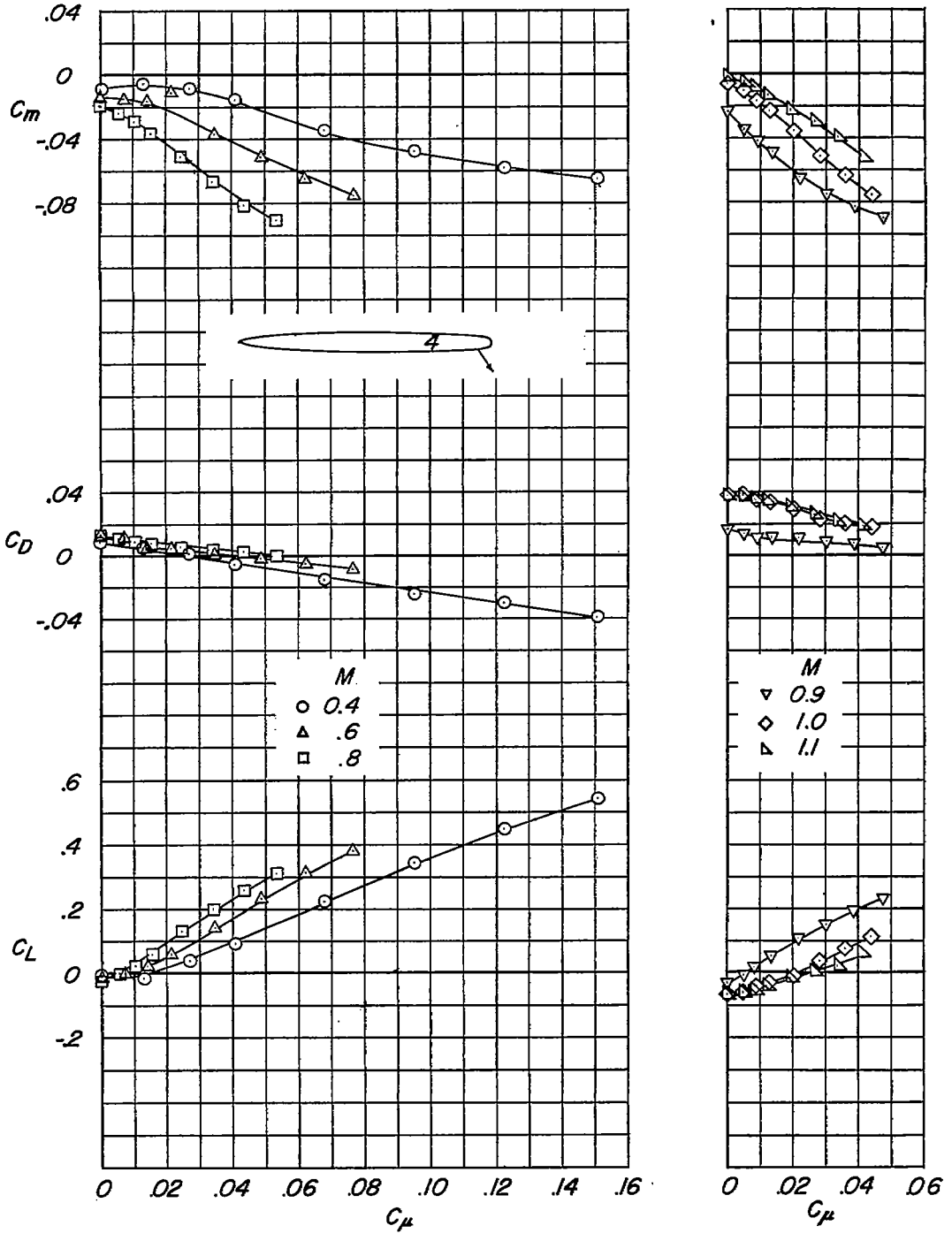

Figure 12.- Effect of Mach number on aerodynamic characteristics of jet-flap model 4. $\alpha = 0^\circ$; $\delta = 56^\circ$.

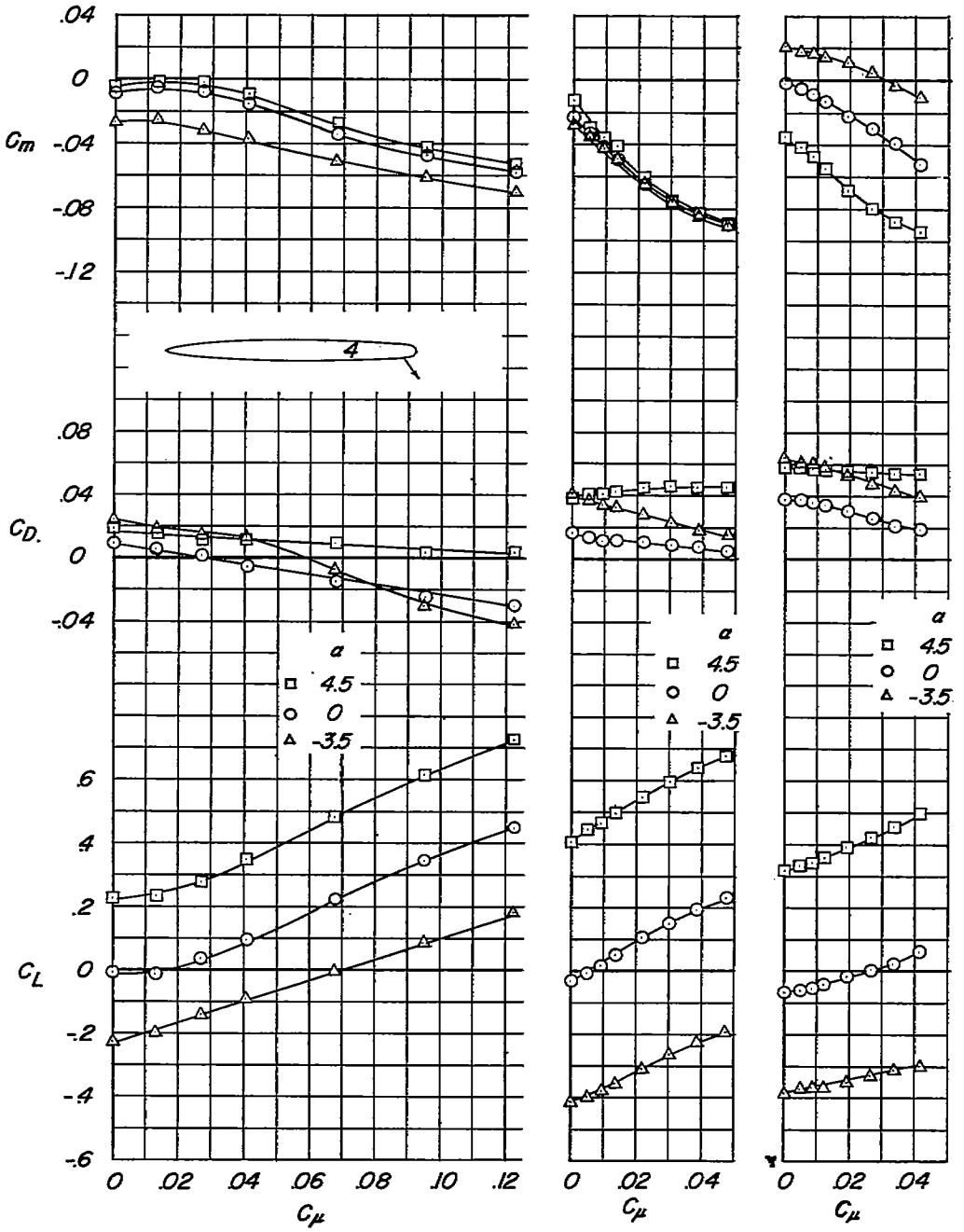

(a) M = 0.40. (b) M = 0.90. (c) M = 1.10.

Figure 13.- Effect of angle of attack on aerodynamic characteristics of jet-flap model 4. $\delta = 56^\circ$.

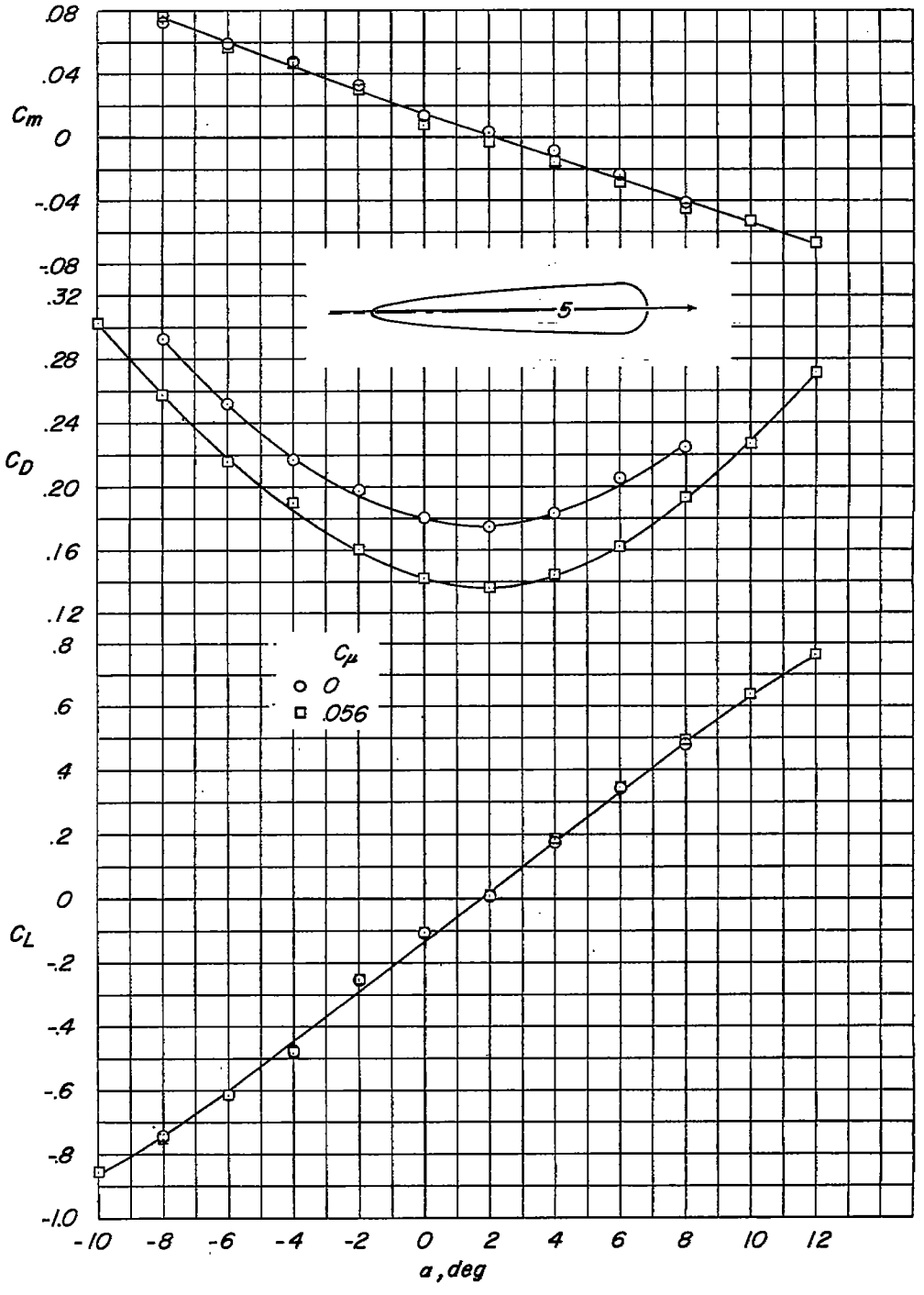

Figure 14.- Effect of momentum coefficient on aerodynamic characteristics in pitch of model 5. $\delta = 0^\circ$; M = 1.10.

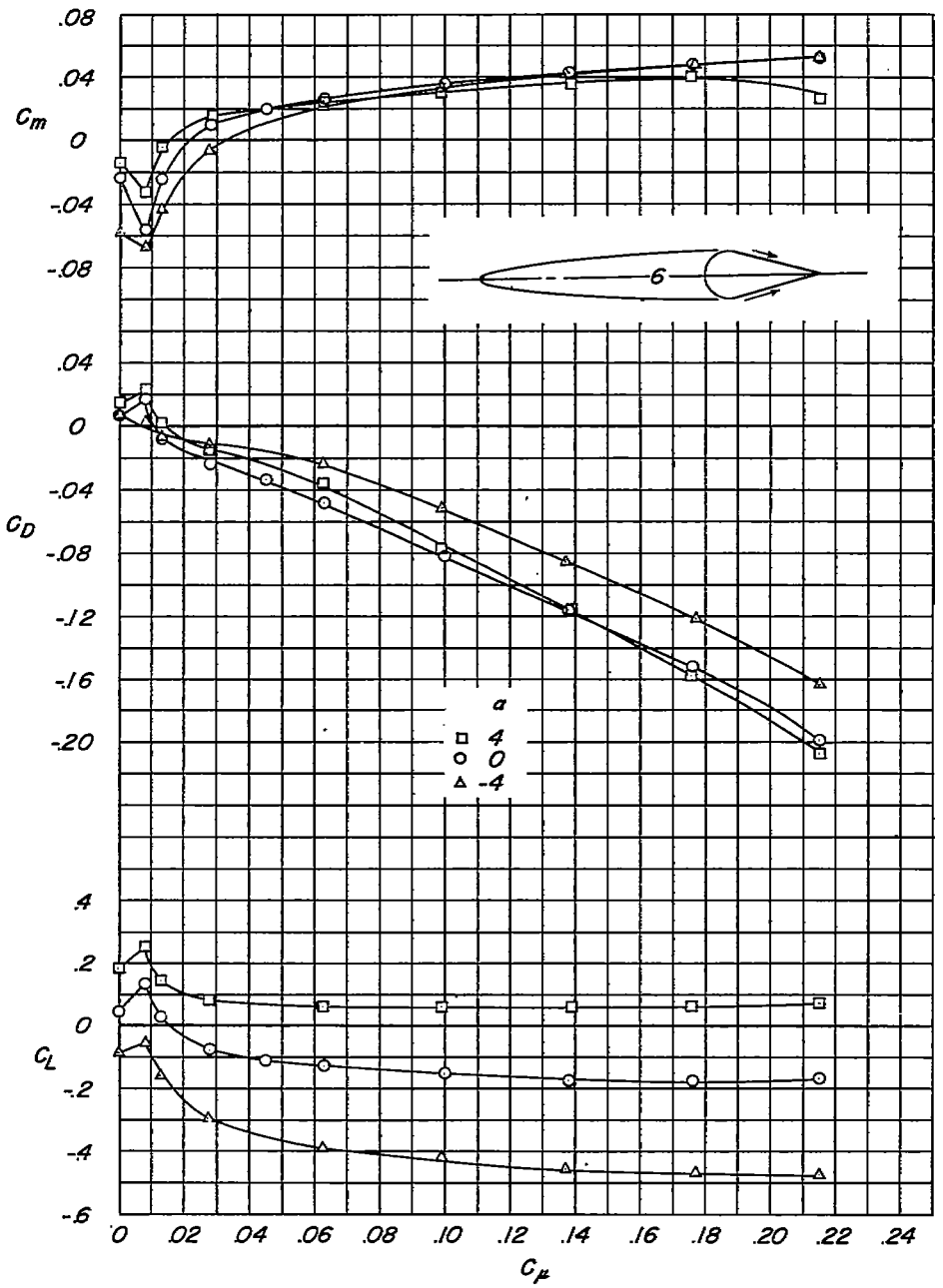

(a) M = 0.40.

Figure 15.- Effect of angle of attack on aerodynamic characteristics of model 6. $\delta = 0^\circ$.

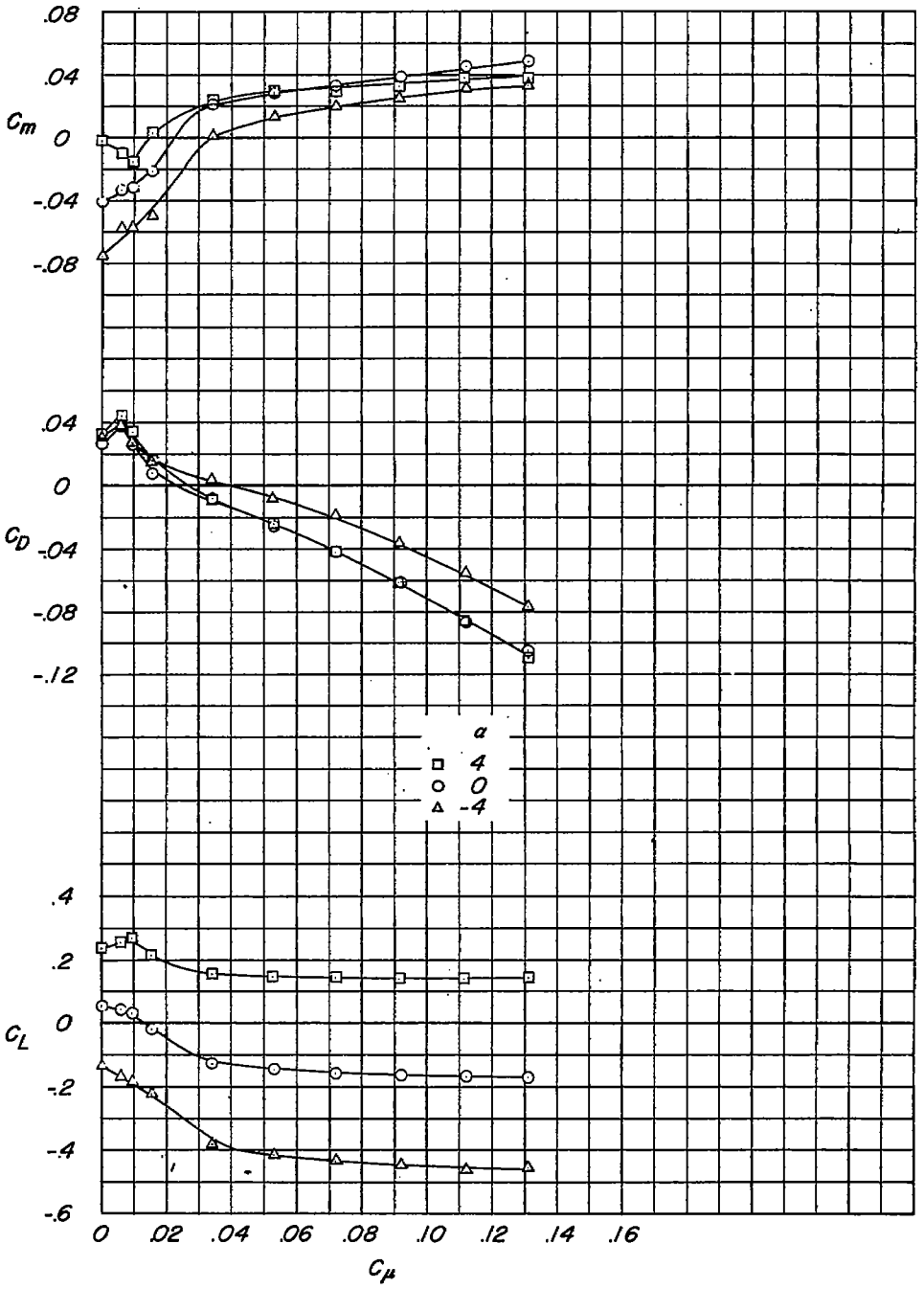

(b) M = 0.60.

Figure 15.- Continued.

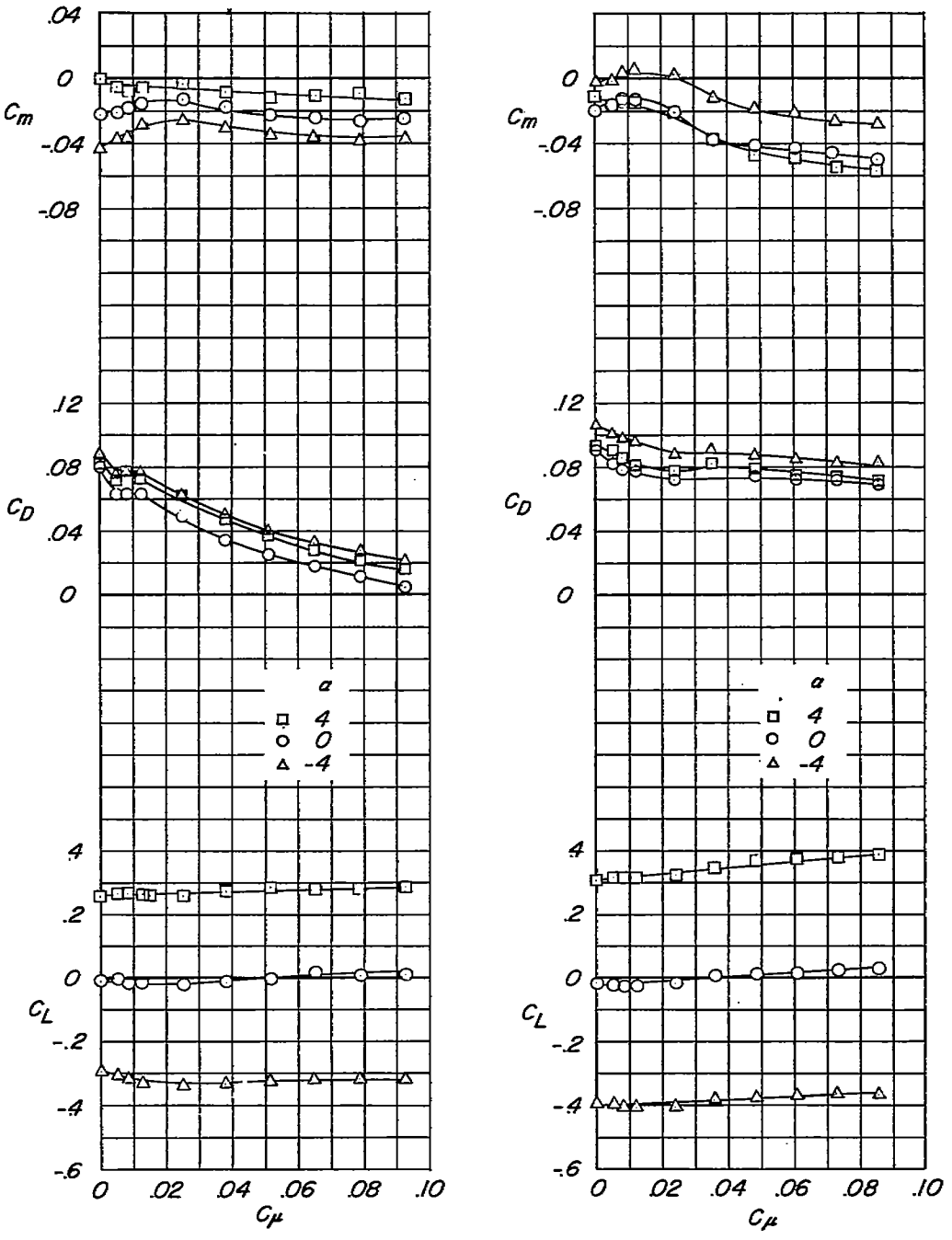

(c) M = 0.80. (d) M = 0.90.

Figure 15.- Continued.

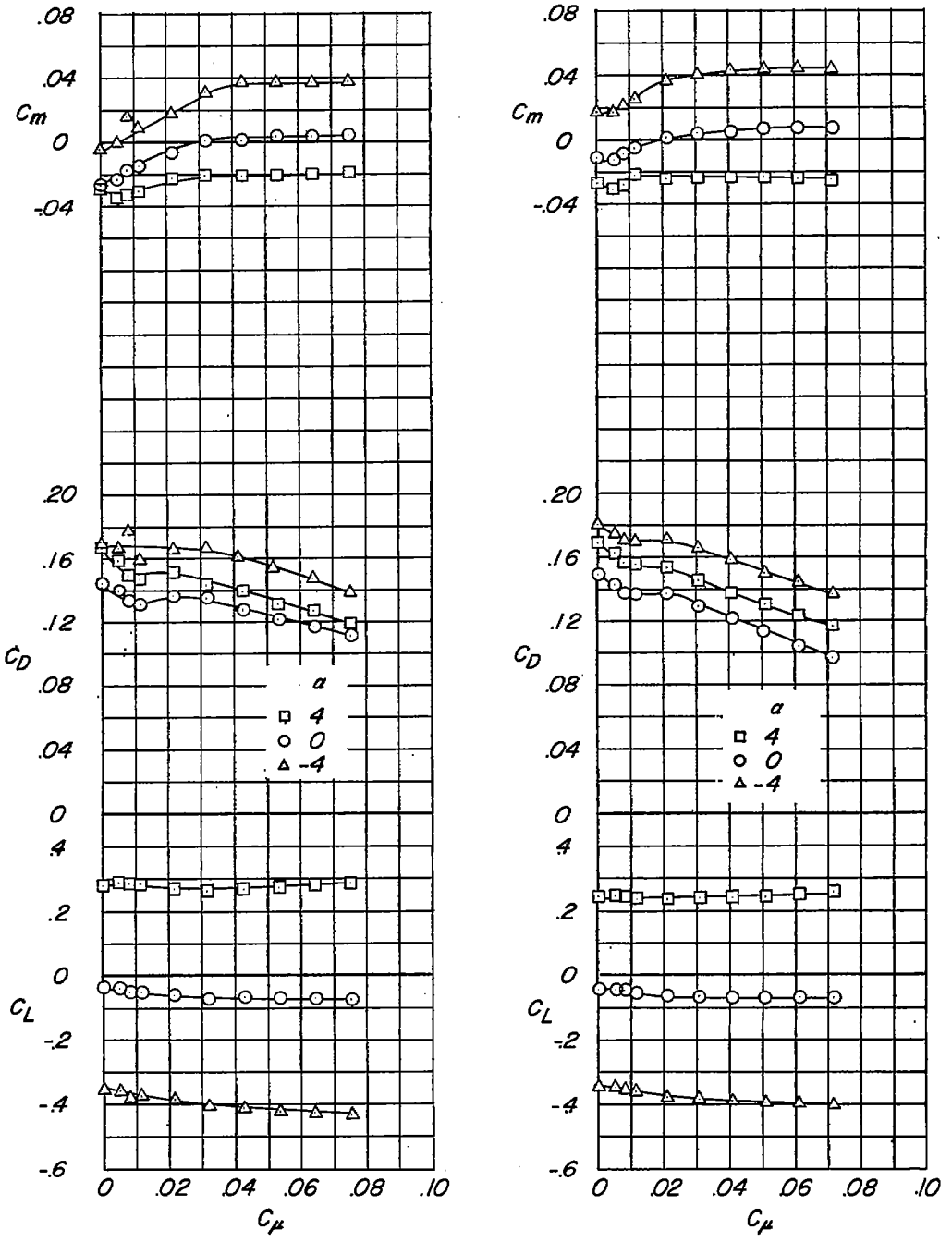

(e) M = 1.00. (f) M = 1.10.

Figure 15.- Concluded.

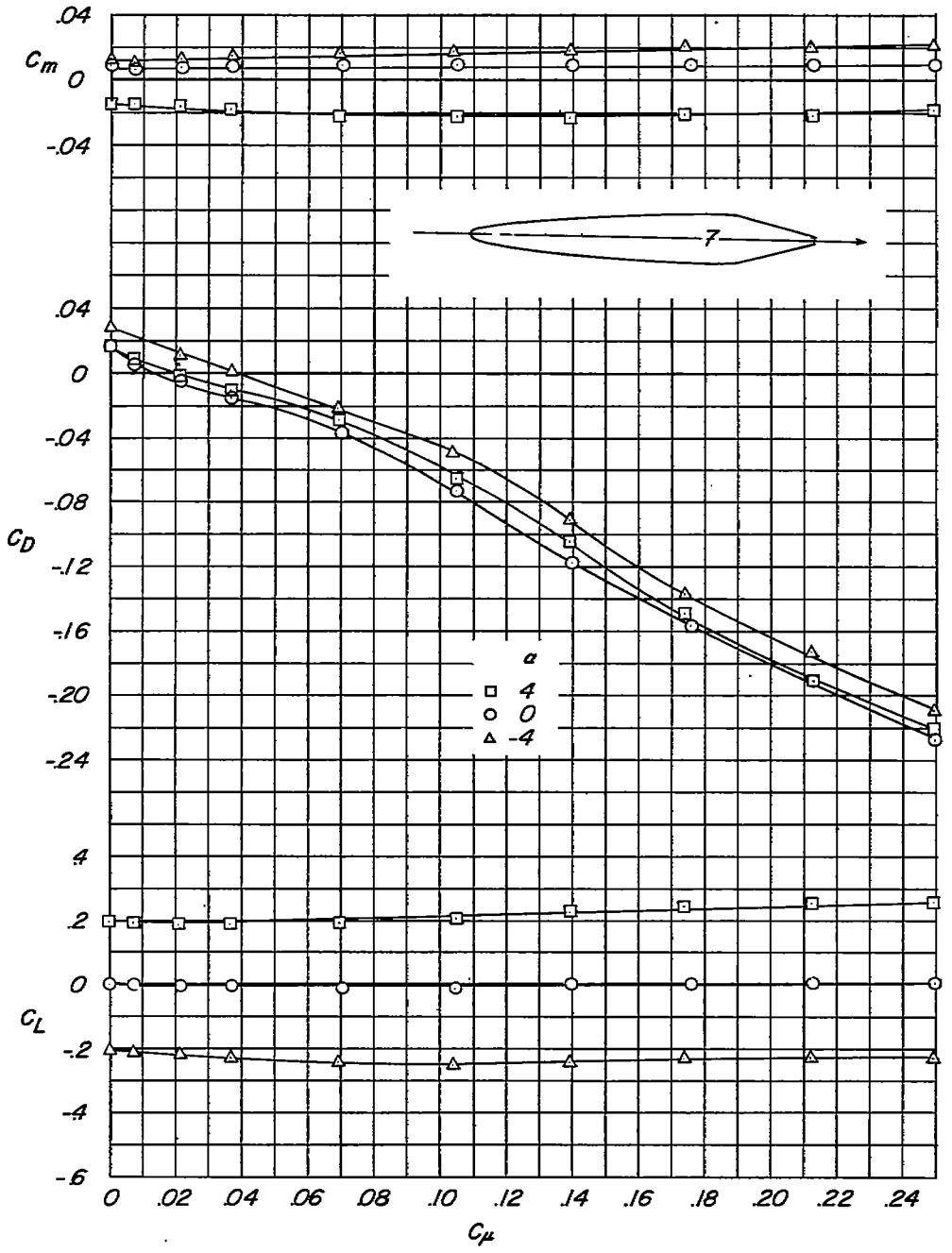

(a) M = 0.40.

Figure 16.- Effect of angle of attack on aerodynamic characteristics of model 7. $\delta = 0^\circ$.

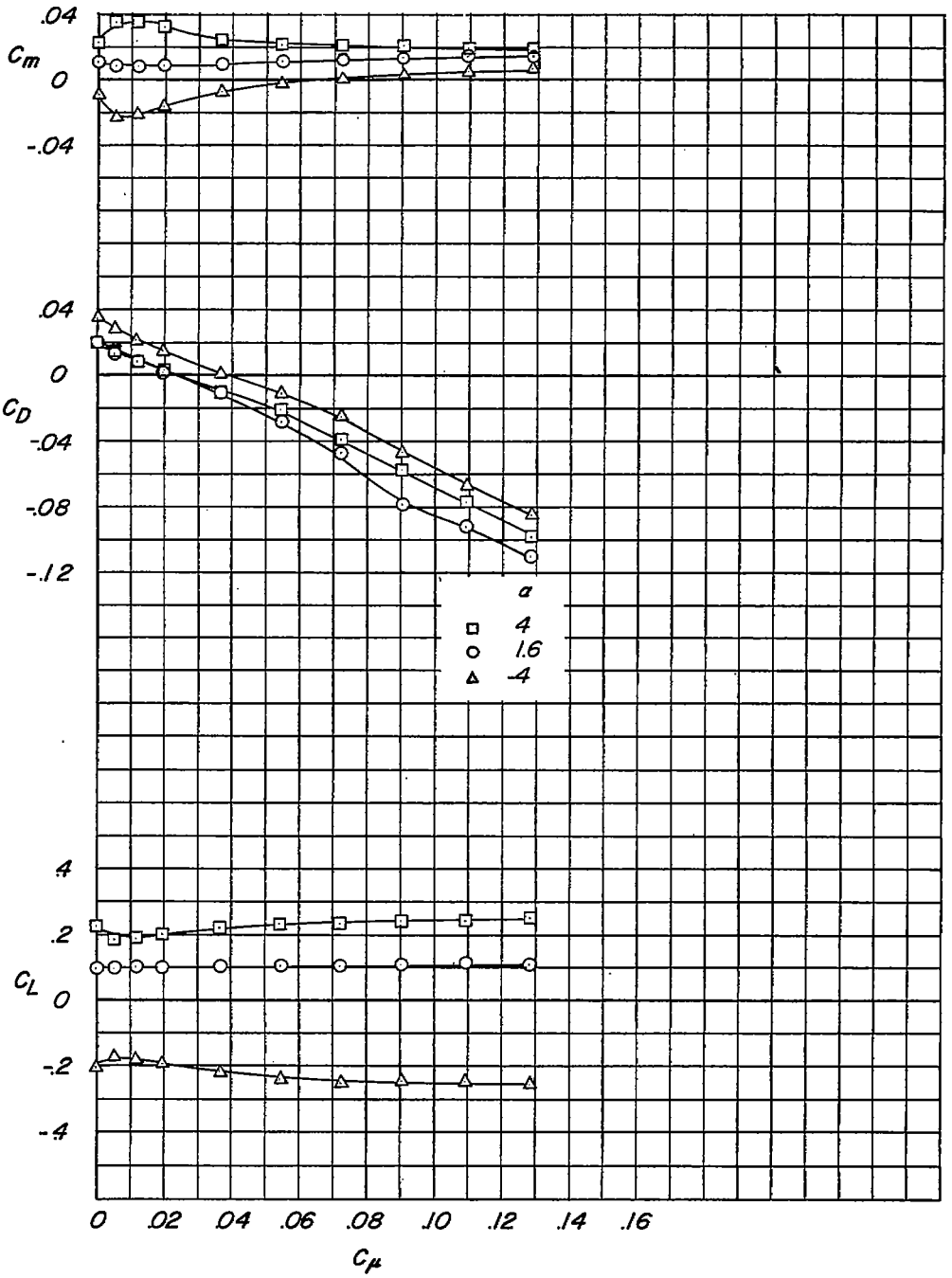

(b) M = 0.60.

Figure 16.- Continued.

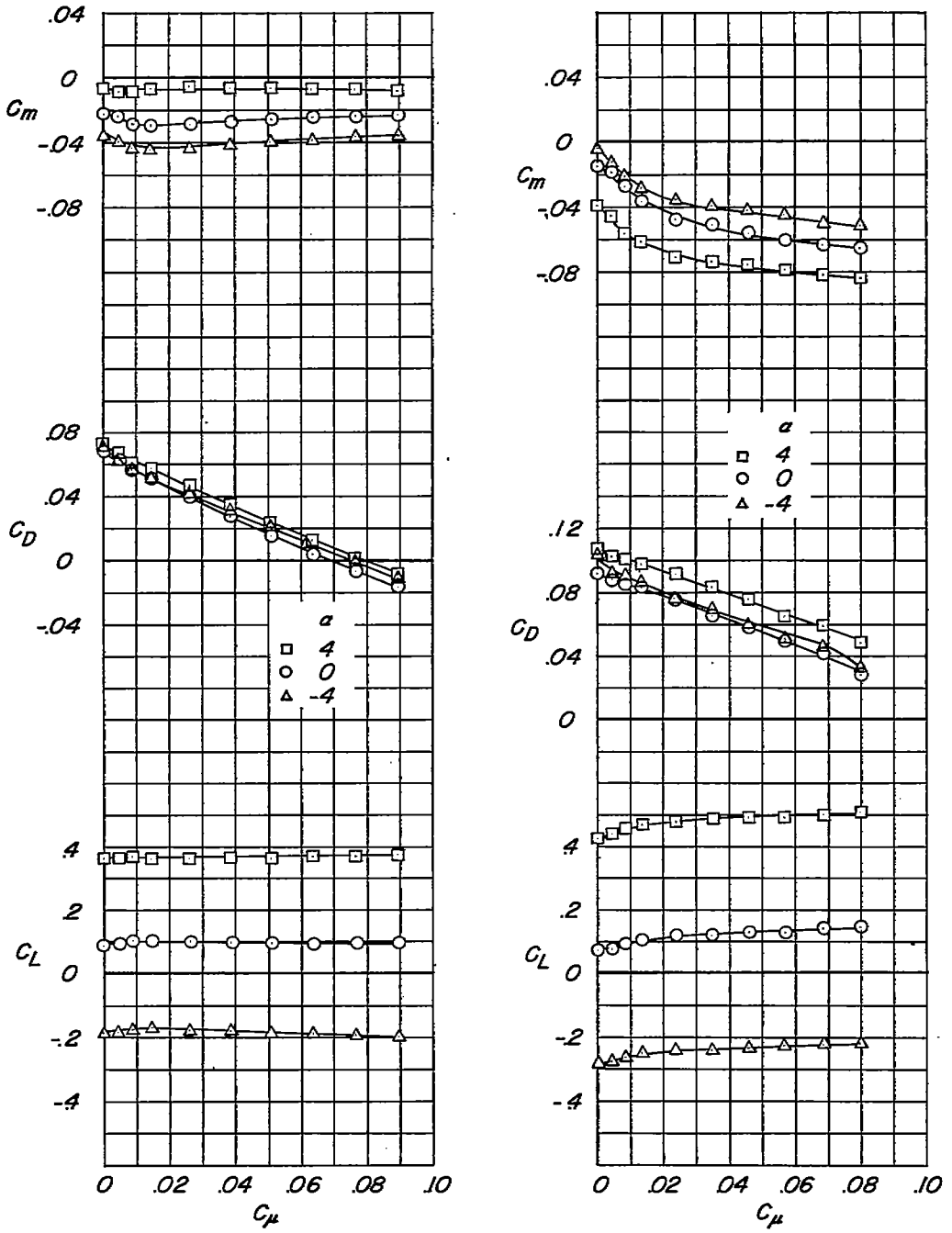

(c) M = 0.80. (d) M = 0.90.

Figure 16.- Continued.

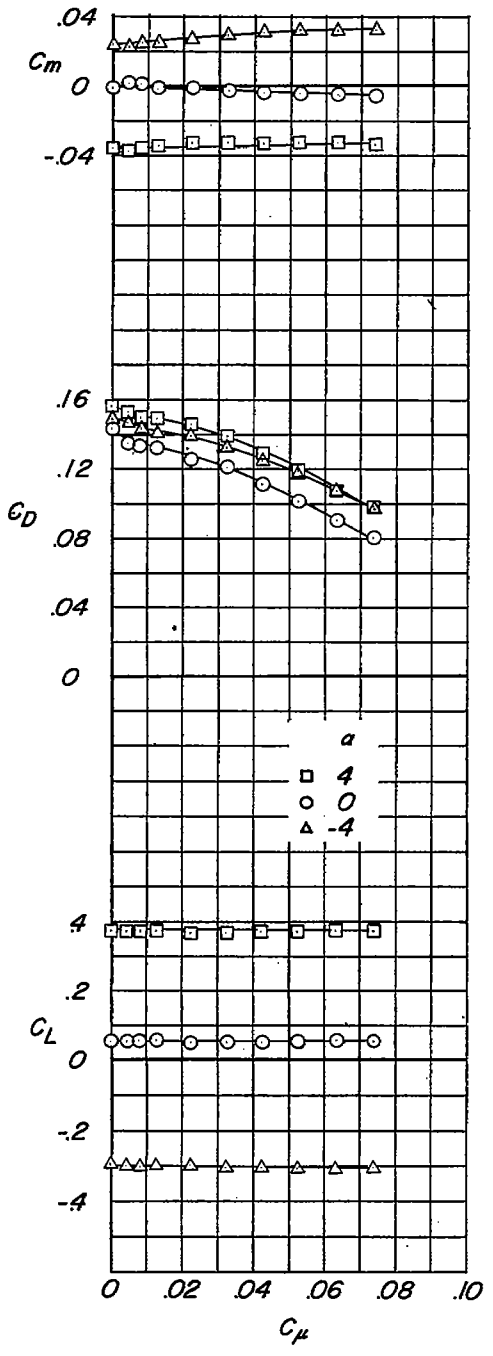

(e) M = 1.00.

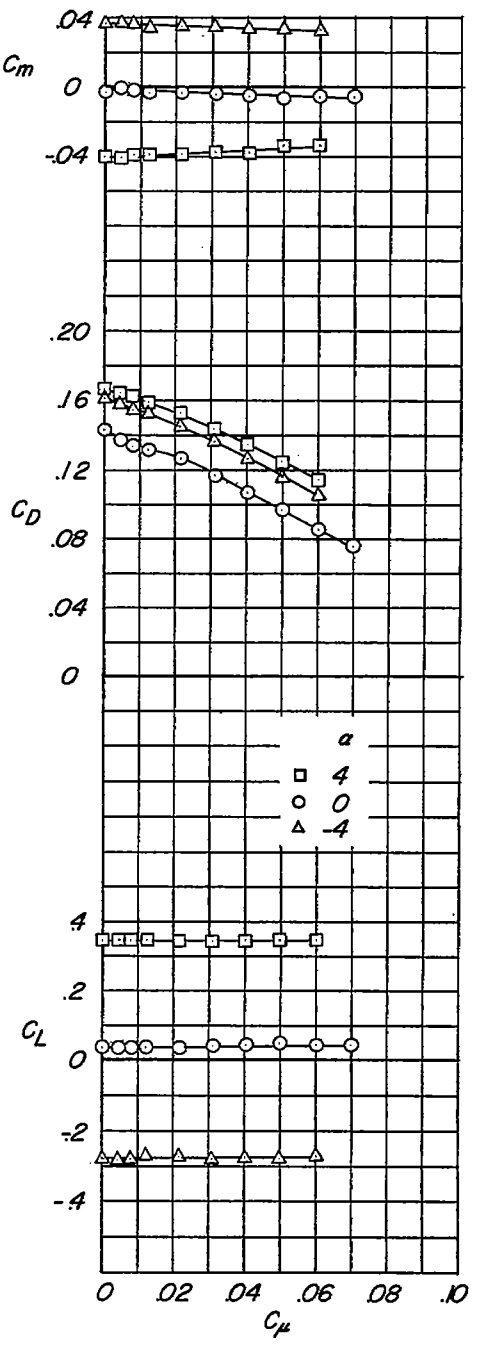

(f) M = 1.10.

Figure 16.- Concluded.

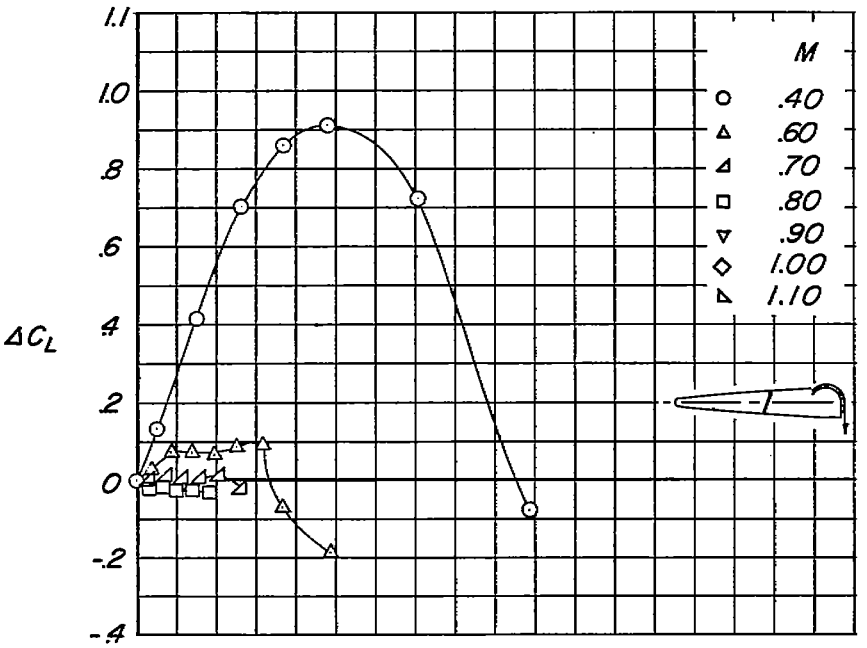

(a) Model 1; $\delta = 79.5^{\circ}$.

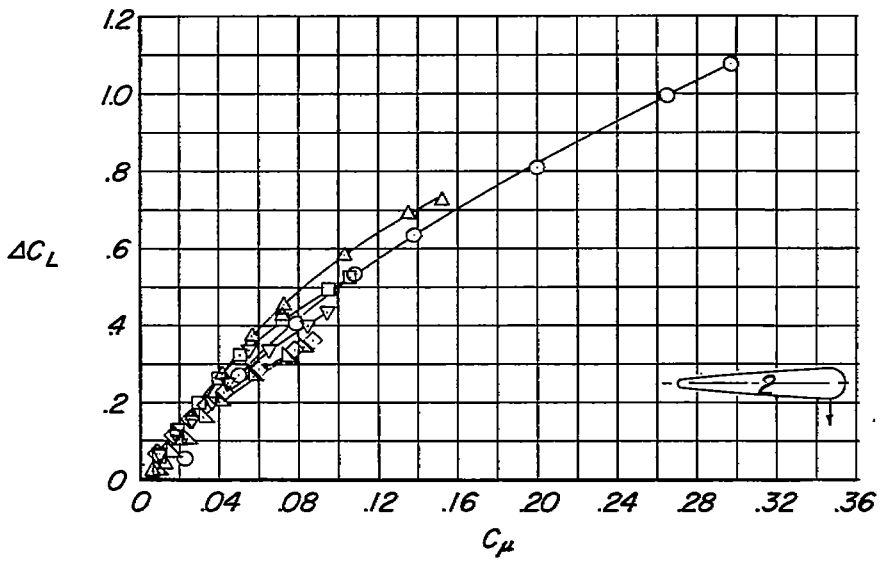

(b) Model 2; $\delta = 90^{\circ}$.

Figure 17.- Effect of Mach number on incremental lift coefficient due to blowing. $\alpha = 0^{\circ}$.

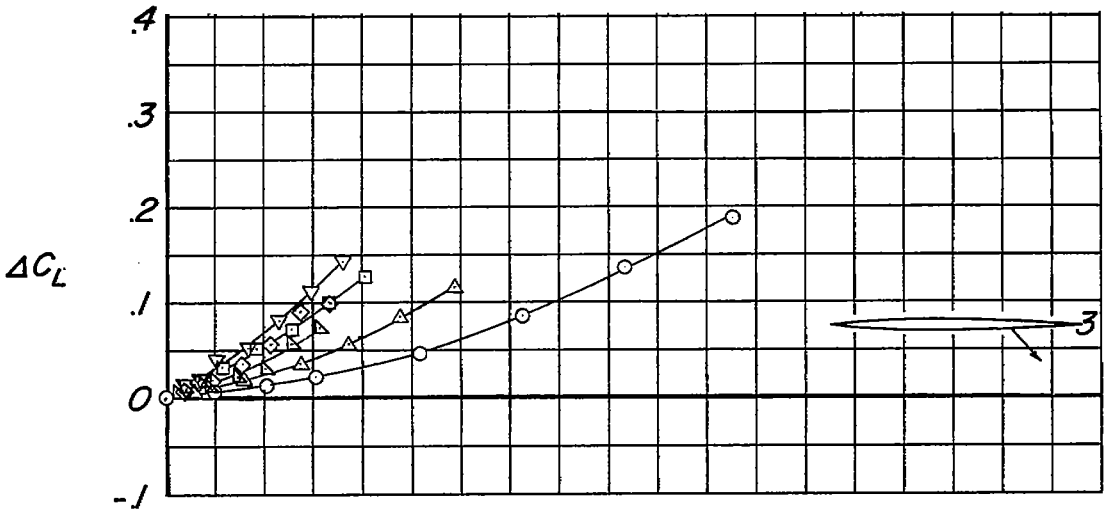

(c) Model 3; $\delta = 50^\circ$.

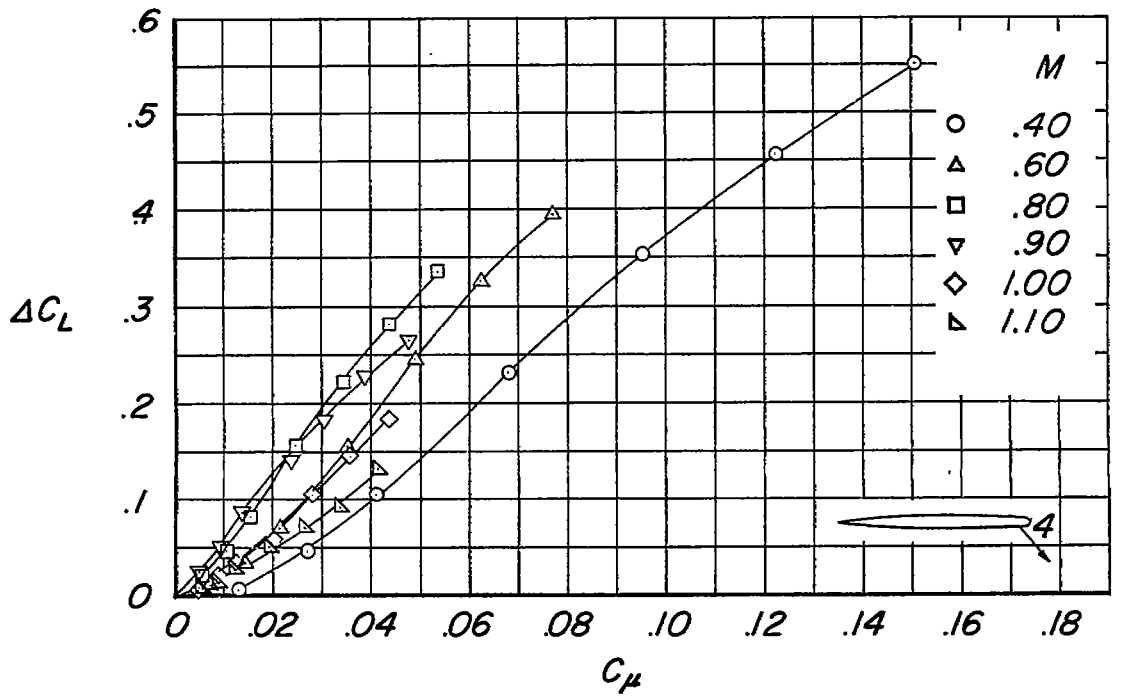

(d) Model 4; $\delta = 56^\circ$.

Figure 17.- Concluded.

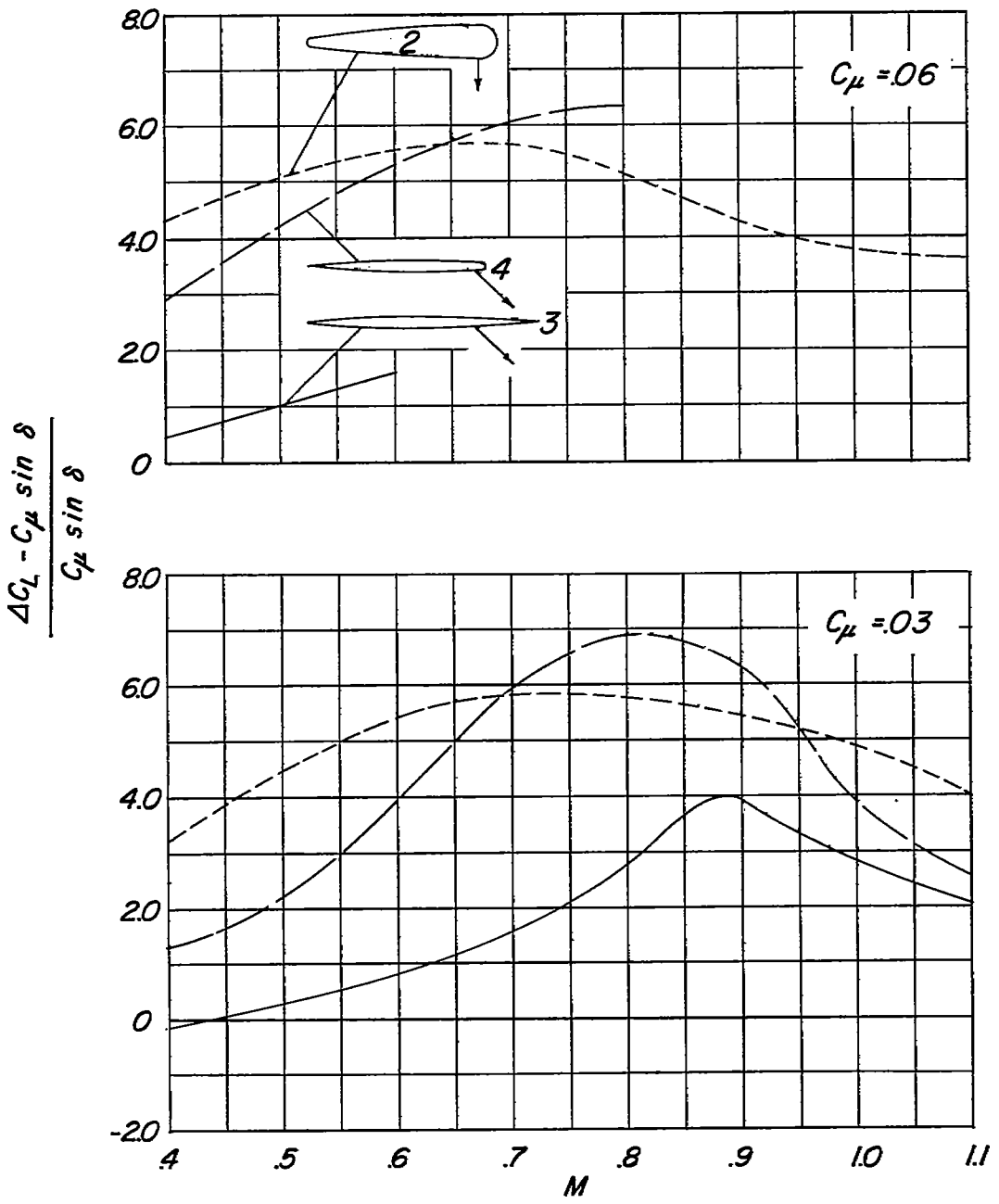

Figure 18.- Variation of lift magnification factor $\frac{\Delta C_L - C_\mu \sin \delta}{C_\mu \sin \delta}$ with M for the lift-augmentation models. $\alpha = 0^\circ$.

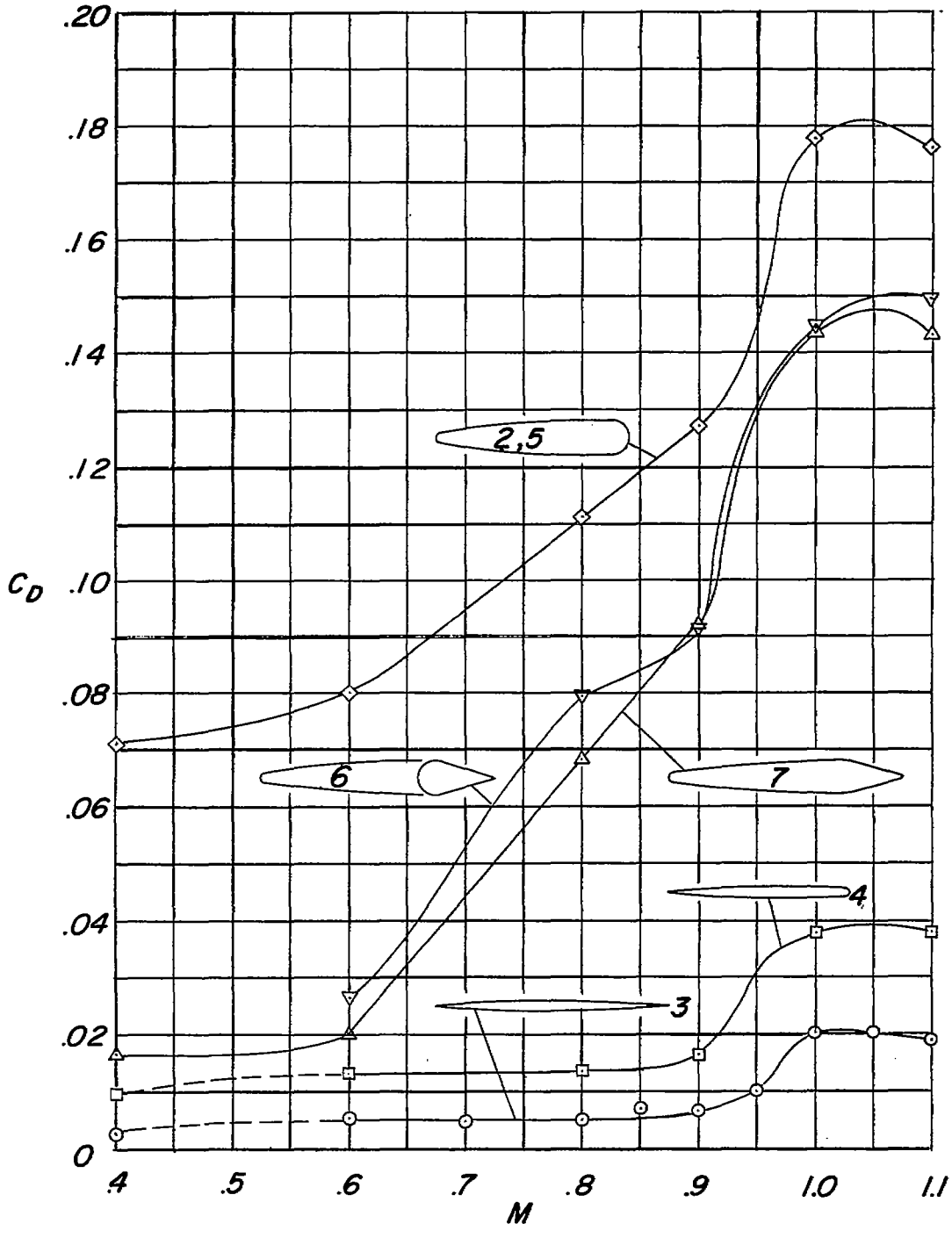

Figure 19.- Variation of C_D with M for several models. $\alpha = 0^\circ$, $C_\mu = 0$.

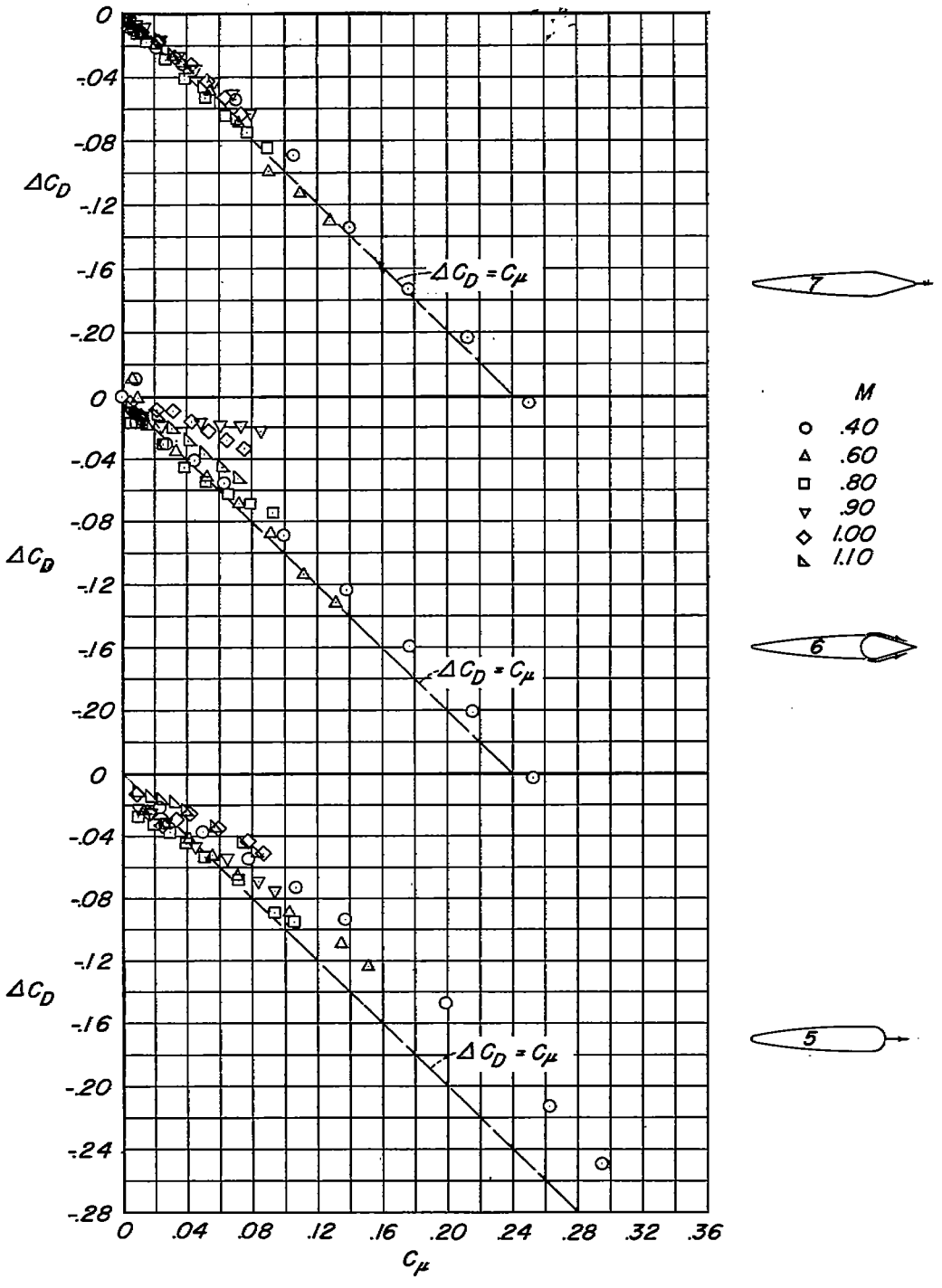

Figure 20.- Effect of Mach number on incremental drag coefficient due to blowing. $\alpha = 0^{\circ}$.